Vibrational Energy Flow in Highly Excited Molecules: Role of Intramolecular Vibrational Redistribution

David J. Nesbitt*,†

Department of Chemistry and Biochemistry, University of Colorado and JILA, National Institute for Standards and Technology and University of Colorado, Boulder, Colorado 80309-0440

Robert W. Field

Department of Chemistry, Massachusetts Institute of Technology, Cambridge, Massachusetts 02139

Received: March 6, 1996; In Final Form: May 30, 1996[⊗]

A pedagogical overview of intramolecular vibrational redistribution (IVR) phenomena in vibrationally excited molecules is presented. In the interest of focus and simplicity, the topics covered deal primarily with IVR in the *ground* electronic state, relying on examples from the literature to illustrate key points. The experimental topics discussed attempt to sample systematically three different energy regimes on the full potential surface corresponding to (i) "low", e.g., moderate- to high-resolution vibrational spectroscopies, (ii) "intermediate", e.g., stimulated emission pumping and high overtone spectroscopies, and (iii) "high", e.g., photofragment/predissociation dynamical spectroscopies. The interplay between experiment and theory is highlighted here because it has facilitated enormous advances in the field over the past decade.

I. Introduction

At the very core of all fundamental chemical transformations is the making and breaking of bonds, yet in most molecular systems beyond simple diatomics this process has proven to be one of the most difficult and challenging to understand dynamically. The reason for this is intimately connected with the nature of highly vibrationally excited states near dissociation and the importance of "intramolecular vibrational redistribution," or IVR, toward which this review is addressed. The impact of IVR phenomena in all of chemistry[1−9] can hardly be overstated and is at the heart of any first principles description of rates of chemical reactions.[10,11] Although particularly stunning progress in this field has recently been possible through technological advances in both experiment and theory, an appreciation of the importance of IVR is nearly as old as *The Journal of Physical Chemistry* itself and therefore an eminently appropriate topic for a pedagogical overview in this 100th-year issue.

One simple way to see why IVR and chemistry are so intimately connected is shown schematically in Figure 1, which displays a typical reaction coordinate diagram for transformation between reactants and products. Near the regions of the potential energy surface corresponding to reactants and products, motion of the nuclei is constrained near local minima, where the restoring forces for sufficiently small displacements are purely *quadratic*. From such a "ball and spring" Hooke's law model of nuclear motion in rectilinear coordinates, we are able to use normal mode analysis and simple quantum mechanical ideas to solve *exactly* for the appropriate linear combinations of nuclear displacements, which correspond to perfectly "uncoupled" harmonic oscillators. Vibrational energy placed in one or several of these oscillators therefore remains localized in a given normal mode. From a time-domain perspective, there is no opportunity in a purely harmonic system for energy to flow from a collective excitation of oscillators into a specific low-frequency mode mimicking a weak bond. On the other hand,

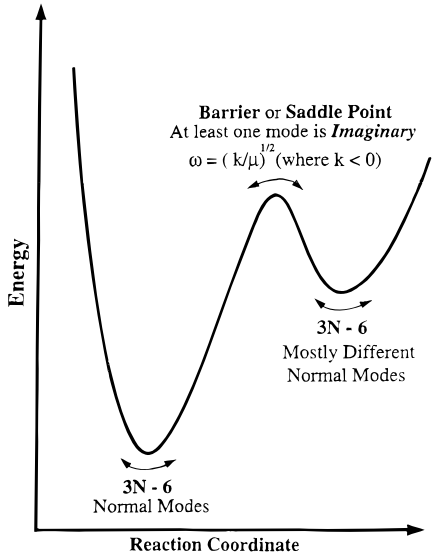

Figure 1. Schematic potential energy cartoon indicating how near-harmonic concepts of vibrational motion (which are often appropriate in the reagent and product well regions) necessarily break down for intermediate stages in the chemical transformation, which is thus the key reason why IVR phenomena play an ubiquitous role in chemistry.

as one systematically proceeds up in energy toward the top of a barrier or out along some dissociation coordinate, this harmonic description begins to break down, both necessarily and catastrophically. Consequently, as is true in many of the most challenging fields of science, what we as chemists seek to understand (i.e., bond breaking and chemical reactions) relies on understanding the systematic "crumbling" of the original paradigm, in this case for nuclear motion as a function of internal energy! Of course, the long-hoped-for "blessing" implicit in this "curse" is that IVR might therefore exhibit sufficient sensitivity to molecular system, energy, and vibrational degree of freedom to allow us to influence and/or control chemical reaction pathways with laser light excitation. Even though this has been largely achieved for relatively small systems such as vibrationally excited triatomics,[12−15] it is fair to say that such a

* To whom correspondence should be addressed.
† Staff Member, Quantum Physics Division, National Institute of Standards and Technology.
⊗ Abstract published in *Advance ACS Abstracts,* July 15, 1996.

S0022-3654(96)00698-3 CCC: $12.00

goal has proven substantially more elusive in larger polyatomics than perhaps was initially appreciated.

Since the key issues of IVR deal with vibrational behavior at chemically significant energies, and which historically have been more easily accessed via visible/UV excitation, the field of IVR has received considerable stimulus from studies of *electronically* excited states.[16−26] From laser-induced fluorescence (LIF) studies, manifestations of IVR as a function of vibrational excitation in S_1, T_1, etc., have been extensively investigated. Since the dynamics occur on electronically excited surfaces, however, there can also be additional interactions due to nonadiabatic radiationless transitions such as internal conversion and intersystem crossing.[19−21,27,28] Although of considerable interest and importance in their own right,[29−31] such electronic effects do not reflect intrinsic IVR dynamics. This has stimulated a particularly heightened interest in spectroscopic probes of IVR phenomena exclusively in the *ground* electronic state manifold, based on techniques such as high-overtone vibrational pumping,[32−50] high-resolution IR absorption spectroscopy in supersonic jets,[51−71] and stimulated emission pumping (SEP) methods.[72−82] Indeed, it is toward IVR dynamics in the ground state that this review is primarily focused, although we also consider relevant examples from the literature on electronically excited states. Of equal importance in this review is the very exciting parallel theoretical efforts[83−100] toward interpreting these ground-state experimental results and, in particular, attempts to develop a more *predictive* understanding of IVR. Our goal is an easily read introduction and overview to IVR phenomena, accessible to people outside of the field, rather than an exhaustive summary aimed at experts. This choice always runs the risk of annoying our closest and most valued colleagues, but in the spirit of this Centennial Issue and in the interest of pedagogy we feel such a risk worth taking.

The organization of this review therefore is as follows. Section II establishes what is meant by IVR, zeroth-order models of the phenomenon, and the spectral and time-domain manifestations of this process. The next three sections discuss selected experimental and theoretical studies of IVR, mostly spectroscopic in nature, that correspond to three different energy regimes on the molecular potential surface. Specifically, section III describes the effects of vibrational excitation relatively *low* in the potential well, where high-resolution IR methods have proven particularly powerful in probing relatively weak IVR mode couplings and correspondingly long-time IVR behavior. Section IV considers *intermediate* excitation of states progressively higher up the potential ladder, such as has been accessed via high-overtone vibrational pumping or stimulated emission pumping and dispersed fluorescence spectroscopies and which can sample much larger regions of the full potential surface. Section V addresses the manifestations of IVR in the *high*-energy limit, where excitation can be above barriers to unimolecular dissociation, isomerization, etc. Section VI discusses the structural dependence of IVR and prospects of predicting or influencing IVR in specific molecular systems. Section VII presents some brief concluding remarks.

II. What Is IVR? A Pedagogical Tool Kit

A. Background. As physical chemists, it is natural for us to think of molecules as a collection of balls and springs. We know that if one spring were to be stretched and then suddenly released, the initial *bond-localized* excitation would spread quickly and in an apparently complex manner over the entire molecular framework (see Figure 2); this is the essential phenomenon of *intramolecular vibrational redistribution*. Three long-standing goals in the study of IVR have been (i) to find a concise language to describe and quantify this complex intramolecular ballet, (ii) to predict the energy flow rates and pathways for any imaginable initial excitation (i.e., dependence on excitation energies, type of bond(s) excited, excitation temporal profile, etc.), and (iii) to extract information about IVR that is encoded in both frequency- and time-domain experiments. More specifically, however, chemists are in the business of making and breaking chemical bonds. If it were possible to insert a chemically significant amount of energy in one bond and keep it there for a chemically relevant time, this could create wonderful possibilities for external manipulations of chemical reactivity. Many such schemes have proven naive, yet the dream of external control[101−108] over chemical processes continues to fuel the study of IVR. IVR has proven a worthy adversary!

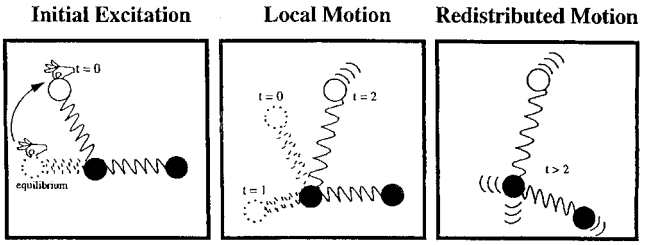

Figure 2. Intuitive classical mechanical "ball and spring" model for IVR, indicating how a localized vibrational excitation inevitably spreads over the entire molecular framework. A description of the detailed time scale and pathway for energy flow of an arbitrary localized vibrational excitation (i.e., the dependence on both location and total excitation energy) is the ultimate goal of any satisfactory model of IVR.

Even though IVR is a simple and ubiquitous concept, it is also extremely subtle and has been made even more difficult by seemingly contradictory descriptions of the process. The key to this semantic difficulty is that the ball-and-spring picture of IVR is inherently *dynamic*, yet below the lowest dissociation level all molecules have sharp, well-resolved energy levels or molecular eigenstates, which are inherently *static*. Even when an eigenstate, ψ_n, which belongs to an energy eigenvalue, E_n, is written as a solution of the time-dependent Schrödinger equation (for a time-independent $\hat{H}$),

$$\hat{H}\Psi(t) = i\hbar \frac{\partial \Psi}{\partial t} = E_n \psi_n e^{-iE_n t/\hbar} \tag{2.1}$$

the probability distribution, $\Psi^*\Psi$, and all expectation values of dynamically relevant quantities (e.g., functions of position or momentum), $\langle \hat{A} \rangle$, are time-independent. Simply stated, the probabilities associated with molecular eigenstates do not move!

The motion associated with IVR arises because the *localized* initial excitations in which we are interested are *not* eigenstates of the molecular Hamiltonian. However, any arbitrary initial state, $\Psi(t=0)$, can always be expressed as a superposition of these eigenstates

$$\Psi(0) = \sum c_i \psi_i \tag{2.2}$$

where

$$c_i \equiv \langle \psi_i | \Psi(0) \rangle \tag{2.3}$$

and for which the time evolution of this initial state is given by the simple prescription

$$\Psi(t) = \sum_i c_i \psi_i e^{-iE_i t/\hbar} \tag{2.4}$$

This non-eigenfunction *does* have a probability distribution that

evolves in time, with the time-dependent probability distribution, $P(\mathbf{Q},t)$, given by

$$P(\mathbf{Q},t) = \Psi^*(\mathbf{Q},t)\,\Psi(\mathbf{Q},t) = \sum_i |c_i|^2 |\psi_i(\mathbf{Q})|^2 + \sum_{i>j} [c_i c_j^* \psi_i(\mathbf{Q}) \psi_j^*(\mathbf{Q}) e^{i(E_j - E_i)t/\hbar} + \text{c.c.}] \quad (2.5a)$$

and a time-dependent autocorrelation given by

$$\langle \Psi(t)|\Psi(0)\rangle = \sum_i |c_i|^2 e^{iE_i t/\hbar} \quad (2.5b)$$

There are several commonly misunderstood points that should be clarified with regard to the initially excited state. First of all, many spectroscopic studies of IVR are conducted with cw, nearly monochromatic lasers. These lasers typically excite eigenstates; they *never* prepare the initially localized excitation with which one associates a time-dependent relaxation. In frequency-domain studies of IVR, it is from the *frequency splittings* (related to E_i) and *relative intensities* (related to $|c_i|^2$) in a high-resolution spectrum that the nature of the initially localized excitation and its subsequent dynamics are inferred. If this initially localized excitation were produced by a suitable laser pulse, then the time-domain behavior of the autocorrelation $\langle \Psi(t)|\Psi(0)\rangle$ would be *exactly* predicted by the results from these frequency-domain experiments. A second point of clarification is that such a short pulse (or pulse sequence) prepares a rather special class of initially localized excitations, which by virtue of its special coupling to the external laser field is referred to as a "zero-order bright state" (ZOBS). Although called a "state", a ZOBS is not a molecular eigenstate; it moves! Since our picture of what the initial vibrational motion looks like (see Figure 2) is rather good at early times, the ZOBS is often labeled by $3N - 6$ vibrational and 3 rotational quantum numbers (J, K_a, K_c). However, most of these quantum numbers correspond to operators which *may not commute* with the exact molecular Hamiltonian, from which the true eigenstates are obtained. As a final note of caution, *the same sets of quantum numbers are often used to label both ZOBS and eigenstates*. This labeling for the eigenstates is, of course, approximate, but it is intended to provide useful labels that express the dominant (or *nominal*) character of that eigenstate.

B. An Example. An explicit example may help solidify these concepts. Consider, for example, a 2:1 bend−stretch anharmonic term in the potential energy function $V(Q_1,Q_2,...,Q_{3N-6}) \equiv V(\mathbf{Q})$, namely $k_{1,22}\,\hat{Q}_1\hat{Q}_2^2$. In a product basis of harmonic oscillator functions (i.e., our zero-order picture), this term will couple modes 1 and 2, following the selection rule $2\Delta v_1 = -\Delta v_2$ (with $\Delta v_i = 0$ for all other normal modes) by a matrix element that scales rigorously as[109]

$$\langle v_1{-}1, v_2|k_{1,22}\hat{Q}_1\hat{Q}_2^2|v_1, v_2{-}2\rangle \propto v_1^{1/2}[v_2(v_2-1)]^{1/2} \quad (2.6)$$

Each vibrational basis state, which has the form

$$\Phi^\circ_{v_1,...,v_{3N-6}}(Q_1,...,Q_{3N-6}) = \prod_{i=1}^{3N-6} \phi_{v_i}(Q_i) \quad (2.7)$$

belongs rigorously to a set of $3N - 6$ vibrational quantum numbers. These basis states are mixed by the bend−stretch anharmonic interaction to yield vibrational eigenstates, which are perhaps misleadingly (but still usefully) labeled by the same $3N - 6$ vibrational quantum numbers. For the above example, the $|1,0\rangle$ and $|0,2\rangle$ basis states mix to form the "$|1,0\rangle$" and "$|0,2\rangle$" eigenstates

$$\text{"}|1,0\rangle\text{"} = \cos(\theta)|1,0\rangle + \sin(\theta)|0,2\rangle \quad (2.8a)$$

$$\text{"}|0,2\rangle\text{"} = -\sin(\theta)|1,0\rangle + \cos(\theta)|0,2\rangle \quad (2.8b)$$

In eqs 2.8a,b, θ is the mixing angle calculated from the ratio of (i) the off-diagonal matrix element $V = \langle 1,0|\,\hat{H}|0,2\rangle$ (obtained from eq 2.6) to (ii) the difference in zero-order energies,

$$\Delta E^\circ = E^\circ_{10} - E^\circ_{02} = 2\Delta \quad (2.9a)$$

$$E^\circ_{v_1 v_2} = \hbar[\omega_1(v_1 + {}^1/_2) + \omega_2(v_2 + {}^1/_2)] \quad (2.9b)$$

by $\tan(2\theta) = V/\Delta$. This is equivalent to solving the 2×2 secular determinant

$$\begin{vmatrix} E^\circ_{10} - E & V \\ V & E^\circ_{02} - E \end{vmatrix} = 0 \quad (2.10)$$

which yields the true molecular eigenenergies

$$E_\pm = \pm[\Delta^2 + V^2]^{1/2} + \bar{E}^\circ \quad (2.11)$$

where $\bar{E}^\circ$ is the average of the zero-order energies, $\bar{E}^\circ = (E^\circ_{10} + E^\circ_{02})/2$.

Now suppose that we excite this molecule from its vibrational ground state, $|0,0\rangle$, to the energy region of the ν_1 fundamental by using a light pulse that is sufficiently short to overlap both the $E_+ \leftarrow E^\circ_{00}$ and $E_- \leftarrow E^\circ_{00}$ transitions, but not so short as to overlap other zero-order transitions such as ν_2, $2\nu_1$, $3\nu_2$, etc. Suppose also that $|1,0\rangle$ is a "bright state" and $|0,2\rangle$ is a "dark state"; i.e., $|1,0\rangle \leftarrow |0,0\rangle$ (ν_1) is an electric-dipole-allowed infrared transition, and the overtone transition $|0,2\rangle \leftarrow |0,0\rangle$ ($2\nu_2$) is forbidden (or so much weaker as to be negligible). At $t = 0$, the system will therefore be in the ZOBS (for notational convenience we choose $\alpha \equiv \sin(\theta)$ and $\Delta E^\circ > 0$),

$$\Psi(0) = |1,0\rangle = (1-\alpha^2)^{1/2}\text{"}|1,0\rangle\text{"} - \alpha\text{"}|0,2\rangle\text{"} \quad (2.12)$$

which will explicitly evolve in time according to

$$\Psi(t) = (1-\alpha^2)^{1/2}\text{"}|1,0\rangle\text{"}e^{-iE_+t/\hbar} - \alpha\text{"}|0,2\rangle\text{"}e^{-iE_-t/\hbar} \quad (2.13)$$

Since we are interested in energy flow out of the initial ZOBS, a particularly relevant quantity to consider is the square modulus of the time-dependent overlap (or autocorrelation) of $\Psi(t)$ with $\Psi(t{=}0)$, given by

$$|\langle \Psi(t)|\Psi(0)\rangle|^2 \equiv P_{10,10}(t) = [1 - 2\alpha^2 + 2\alpha^4] + 2(1-\alpha^2)\alpha^2 \cos[(E_+ - E_-)t/\hbar] = 1 - (2\alpha^2 - 2\alpha^4)[1 - \cos\omega t] \quad (2.14)$$

where $\omega = (E_+ - E_-)/\hbar$. The system starts out with unit probability in $|1,0\rangle$ at $t = 0$ and reaches a minimum probability in $|1,0\rangle$ at $t = \pi/\omega$, given by

$$P_{10,10}(\pi/\omega) = 1 - 4(\alpha^2 - \alpha^4) = \cos^2(2\theta) \quad (2.15)$$

When $\theta = \pi/4$ (i.e., $\Delta = 0$), the initial state mixing is complete, and the system oscillates from the pure $|1,0\rangle$ state at $t = 0$, $2\pi/\omega$, ..., $2n\pi/\omega$ to the pure $|0,2\rangle$ state at $t = \pi/\omega$, ..., $(2n+1)\pi/\omega$. This simple description correctly predicts the early time dynamics observed in, for example, quantum beat spectroscopies[6,22−26,110,111] and isolated anharmonic resonances, where only two states contribute to the time dependence. This

can, of course, be generalized to dynamics in a state space consisting of far more than two levels, where the time dependence is understandably more complicated but predicted by exactly the same formalism.

One particularly useful second limit to consider is that of a dense manifold of nearly equally coupled levels, with an average state density, ρ, and root mean square off-diagonal matrix element, $\langle V^2\rangle^{1/2}$. In this limit, the square modulus of the autocorrelation $|\langle\Psi(t)|\Psi(t=0)\rangle|^2$ decays approximately[29] as $e^{-\Gamma t}$, with an exponential rate Γ given by the Fermi Golden Rule expression[112]

$$\Gamma = 2\pi\langle V^2\rangle\,\rho \tag{2.16}$$

Many authors make distinctions between dynamics in a low-dimension state space (quantum beats, simple anharmonic resonances, restricted IVR) and a high-dimension state space (multiple overlapping resonances, dissipative IVR, quantum chaos); for the purposes of this discussion, we will not make such distinctions.

In summary, the simplest way of describing the dynamics of IVR is therefore (i) a short-pulse excitation prepares the system in a ZOBS, (ii) the nature of the ZOBS is determined by the nature of the preparation process, and (iii) the dynamics are most readily seen as *motion in state space* (periodic or more complicated), rather than the $3N$ atomic coordinates and $3N$ momenta in phase space. (iv) This motion is described by Fourier components corresponding to eigenenergy differences $[\omega_{ij} \equiv (E_i - E_j)/\hbar]$ and amplitudes corresponding to products of mixing coefficients, which in principle can be obtained from *either* frequency- or time-domain studies.

C. Generic Classes of Bright States. For each molecule, an infinite number of initial states, $\Psi(0)$, with nearly the same value of $\langle E\rangle$ could be prepared, with these initial preparations exhibiting quantitatively and qualitatively different dynamics. However, the experimentalist either cannot or does not have the time to look at more than a few of these possible $\Psi(0)$ initial states; the goal is to learn enough about $V(Q)$ to have a predictably robust theory, i.e., so that consideration of a sufficiently similar initial excitation will result in no large surprises. The choice of $\Psi(0)$ is usually dictated by the nature of the excitation scheme. Historically, these have come in three generic categories: (i) direct vibrational excitation, (ii) Franck−Condon pumping via an electronic transition, and (iii) two-step pumping. A wide variety of such schemes exist, and many exploit supersonic jet cooling and/or double resonance to produce excitation of a $\Psi(0)$ with a single, rigorously known value of each good quantum number, such as total angular momentum and rovibronic symmetry.

One-photon direct vibrational excitation selects a ZOBS which has the largest transition probability from the ground state (i.e., $|0\rangle$) to any of the zero-order states in a specified energy region. This selectivity is based on vibrational selection rules for transitions between basis states which are simple products of $3N - 6$ normal mode (harmonic) oscillator states: strong infrared transitions are $\Delta v_i = \pm 1$, fundamentals (and hot bands) for the normal modes (ν_i) in which the electric dipole moment, μ, varies with the normal coordinate displacement, $\partial\mu/\partial Q_i \neq 0$, and where $\Delta v_j = 0$ for all other modes.[113,114] When one allows for mechanical anharmonicity (the nonvanishing of third and higher derivatives of $V(\mathbf{Q})$ with respect to normal coordinates) and electronic anharmonicity (the nonvanishing of second and higher derivatives of μ with respect to normal coordinates), these vibrational selection rules relax to become propensity rules. As a crude rule of thumb for hydride stretches,[49,115] the intensities of vibrational overtone and combination transitions are exponentially decreasing functions of the total change of vibrational quantum number, ΔV,

$$\text{intensity} \propto 10^{-\Delta V} \tag{2.17a}$$

where

$$\Delta V \equiv \sum_k |\Delta v_k| \tag{2.17b}$$

The drop-off for the first few quanta of excitation may be even steeper[115] by another factor of 10. This means that, in any spectral interval, the strongest vibrational transitions from the $|0\rangle$ level will generally correspond to the smallest ΔV and the greatest anharmonicity. Historically, the states most experimentally accessible by such direct pumping schemes have been the highest frequency and most anharmonic modes, typically built on fundamentals or overtones of an R−H stretch. It is worth noting that this essentially experimental constraint has led to a particular focus on IVR dynamics in H-stretching states, which may or may not be representative of IVR in general. It is therefore quite important that multiple resonance and SEP schemes are now beginning to provide access to a much wider region of the potential surface than the R−H stretches alone.

Another example of the ZOBS concept is commonly seen in weakly bound clusters,[116−126] where even a fundamental vibrational excitation of the subunits often lies well above the cluster's dissociation limit. Therefore, the ZOBS is embedded in and coupled to the continuum of "dark" levels associated with the intermolecular bond dissociation coordinate. Hence, a classic measure of IVR is obtained via Fermi's Golden Rule (eq 2.16) from the predissociation line width of the ZOBS and from the widths of other features (associated with dark states where the intermolecular modes are below the dissociation threshold) that borrow their spectral intensity from the ZOBS and their width from the intermolecular continuum. This kind of experiment provides information about three classes of IVR: bright → dark, bright → continuum, and dark → continuum. Since one of the key observables in such an experiment is the width of features in the frequency-domain spectrum or fluorescence decay rates in a time-domain experiment, it is essential that each feature contain only a single rotational transition (i.e., the feature is *homogeneously* broadened). If several rotational transitions are unresolved (i.e., the feature is *inhomogeneously* broadened), the effective line width does not provide information unambiguously relevant to the IVR dynamics. Double-resonance and/or supersonic jet rotational cooling schemes are often essential to remove these inhomogeneities.

In molecular systems with bound electronic states, *Franck−Condon pumping* followed by either dispersed fluorescence or stimulated emission pumping (SEP) can be used to probe IVR in the ground state. For the initial vibronic excitation step, the relative intensity pattern is determined by the Franck−Condon principle. The Franck−Condon-active vibrational normal modes (those in which $\Delta v_i \neq 0$ transitions can be quite strong) are those that correspond to large changes in equilibrium geometry ($\Delta Q_i^e \neq 0$), frequency ($\Delta\omega_i \neq 0$), and/or form of the normal coordinate.[127] Due to changes in ground vs excited state potential surface topography, the classes of vibrational states accessible via Franck−Condon pumping are often quite different from those accessible via direct vibrational excitation. For example, in the acetylene $\tilde{X}^1\Sigma_g^+$ electronic ground state, the infrared-active normal modes are the antisymmetric C−H stretch (ν_3'') and the *cis*-bend (ν_5''); hence, the small-ΔV propensity rule weighs heavily in favor of ZOBSs which are odd quanta

overtones or combination bands of ν_3'' or ν_5'' built on totally symmetric modes. In contrast, the excited $\tilde{A}$ state is *trans*-bent with a C=C double bond, whereas the $\tilde{X}$ state is linear with a C≡C triple bond; thus, for the $\tilde{A}\ ^1A_u \rightarrow X^1\Sigma_g^+$ electronic transition, the strongly Franck−Condon-active modes are the C−C stretch (ν_2'') and the *trans*-bend (ν_4''). Consequently, by SEP from different vibrational levels in the intermediate $\tilde{A}$ state, one can systematically vary the nature of the $\tilde{X}$ state ZOBS. This extra flexibility can provide new insights into IVR, especially by separating spectrally overlapping features that belong to two different ZOBSs.[78]

Even greater flexibility in the ZOBS selection process can be obtained via *two-step pumping*, based on either sequential vibrational transition steps or the combination of a direct vibrational and Franck−Condon pumping scheme. For example, in acetylene, if one were first to excite fundamentals or overtones in either the antisymmetric CH stretch (k quanta of ν_3'') or the *cis*-bend (r quanta of ν_5''), then Franck−Condon pumping would provide access to the large manifold of ZOBSs of the form

$$|v_1'' = 0, v_2'' = n, v_3'' = k, v_4'' = m, v''_5 = r\rangle$$

for arbitrary n, m. Similarly, in molecules with many nearly degenerate bond-stretching modes (e.g., CH stretches in hydrocarbons), multiple-step pumping methods can be used to prepare qualitatively different distributions of vibrational quanta at nearly the same total energy. For example, in a molecule with two such modes, states with $nv_1 + mv_2$ quanta are more readily accessed by two-step overtone excitation,

$$|0,0\rangle \xrightarrow{\Delta v_1 = n} |n,0\rangle \xrightarrow{\Delta v_2 = m} |n,m\rangle$$

Since the direct anharmonic coupling matrix elements between the two modes, $Q_1^k Q_2^l$, scale as $v_1^{k/2} v_2^{l/2}$, one might expect the v_1/v_2 coupling effects to be most visible in a $|v_1 = 3, v_2 = 3\rangle$ ZOBS than in either $|v_1 = 6, v_2 = 0\rangle$ or $|v_1 = 0, v_2 = 6\rangle$. This would provide a particularly rigorous test of the possible stability of so-called "extreme motion states", where the same total energy is predominantly localized in a specific bond as opposed to excitation of a mode which involves concerted motion of several nuclei distributed throughout the molecule.[56,79−82]

D. Choice of Basis Set. Is IVR a real phenomenon or only a consequence of a poor choice of basis set? Since eigenstates are stationary, one could argue that IVR disappears whenever a frequency-domain spectrum is recorded with resolution sufficient to resolve individual eigenstates. However, this argument is specious because our real-world experience with balls and springs tells us that the underlying dynamics is real and must somehow be reflected in an eigenstate spectrum. To restrict one's reality to the fully resolved transition frequencies and relative intensities is like telling an X-ray crystallographer to stop with the diffraction pattern and not to think about the molecular structure encoded in it!

Ideally, we would know the exact $V(\mathbf{Q})$, which would provide a basis for predicting the dynamics of any conceivable $\Psi(0)$. However, an individual spectrum samples this full potential energy surface through a very narrow aperture and a highly distorting lens. Thus, the study of IVR can be seen as an attempt to extract information about $V(\mathbf{Q})$ by characterizing the dynamics of a small number of selectable ZOBSs. In order to do this, we need to choose an orthonormal basis set with which to describe $\Psi(t)$. One choice of a basis set is the eigenstates, such as revealed by a high-resolution experiment. More physically useful is a basis set typically formed from products of individual vibrational modes, which are related to the eigenstates by an unknown unitary transformation that diagonalizes the molecular Hamiltonian. These basis states could range from localized bond modes, such as would arise in an internal coordinate treatment, to the more delocalized modes from a full normal mode analysis; the "optimum" choice for this non-eigenstate basis is dictated by the nature of the excitation process that prepares the ZOBS. Since the oscillator strength for overtone and Franck−Condon pumping physically arises from a localized initial excitation, and one (in principle if not in fact) excites to the ZOBS using a short pulse of light, $\Psi(t=0)$ is sometimes simplest to represent in a localized bond mode product basis set.[128]

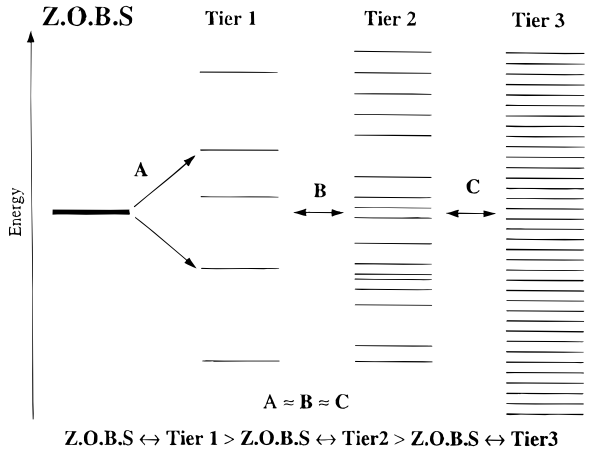

Figure 3. Tier model for analysis of IVR. Energy typically spreads from an initially localized state via strong, low-order anharmonic interactions with a few near-degenerate basis states. These states are in turn each coupled to a successive tier of near-degenerate basis states via additional low-order resonances. The net effect is a hierarchical coupling scheme, sequential energy flow, and a progressive set of tiers with increasing density of states.

IVR is frequently described in terms of tiers of these coupled zero-order states (Figure 3). The physical motivation for this is that the spectrum often naturally reveals hierarchical structures.[83,84,129−133] At the coarsest level of structure is the ZOBS itself. As spectral resolution is increased, the oscillator strength associated with the ZOBS fractionates into finer states, sometimes called "feature" or "doorway" states. As one proceeds systematically from lower to higher resolution, one is able to see more and more states coupled to the ZOBS by progressively weaker and weaker off-diagonal matrix elements of the molecular $\hat{H}$ (expressed in the imperfectly known but complete zero-order basis set).

Sometimes a hierarchical structure is very clear in the spectrum. In such cases a tier structure will be very clear in $\hat{H}$. Typically, each additional tier corresponds to larger values of ΔV away from the ZOBS. For example, the first tier might involve a few strong cubic ($\Delta V = 3$) and quartic ($\Delta V = 4$) anharmonic coupling terms. The second tier would then logically contain states coupled anharmonically to the first tier states ($\Delta V \leq 8$ with respect to the ZOBS) and so on out to higher orders. For $J \neq 0$, the tier structure would also have to include rotationally induced coupling terms due to Coriolis and centrifugal mixing of the basis states.

One could argue that arranging basis states into tiers is an arbitrary and meaningless process. After all, if we do not know explicitly how to define a basis set, how can we be sure that the tiers reflect any real physics? The answer is easily stated but provides little guidance as to how to proceed. If the spectrum contains hierarchical structure, the tiers are real, and

it behooves us to figure out their physical basis. This is not a question of arbitrariness of basis sets related by unitary transformations. The molecule is trying to tell us how to describe the IVR process as a sequence of expansions into larger and larger regions of energetically and symmetry accessible state space.

E. IVR Observables in the Frequency and Time Domain. *Frequency Domain*. In a typical frequency-domain experiment, one attempts to observe and resolve the features that contribute to a specific ZOBS. This ZOBS has an overall width, a countable number of resolved features, an overall intensity, a distribution of level spacings, and a distribution of relative intensities. When the excitation energy is above the lowest dissociation limit, each of the finest features can also have a measurable homogeneous width. By sampling the ZOBS via several preselected $J_{K_aK_c}$ rotational levels, one can obtain rotational constants for the ZOBS, the feature states, and sometimes even the subfeature states. These rotational constants often permit assignment of vibrational quantum numbers. In addition, studies of $J_{K_aK_c}$ dependence can also identify the coupling mechanisms as anharmonic vs Coriolis (a, b, or c type) vs centrifugal.

The information about IVR in a frequency-domain spectrum can be reduced to a generic description or a mechanistic model. At the descriptive level one finds overall measures, such as a hierarchy of widths (or couplings) and a comparison of the observed density of states to various model calculations of the total or restricted (e.g., including only a subset of normal modes) density of states of correct symmetry.[134−136] One also finds statistical measures such as level spacings and intensity distributions (e.g., Δ_3, Σ^2, Brody, χ_ν^2) and hierarchical measures (e.g., parsimonious trees, complexity).[137−139] At the mechanistic level one finds an effective Hamiltonian model that describes all (or most) of the level splittings and relative intensities associated with the ZOBS. This model is expressed in terms of a set of zero-order basis state energies and coupling terms, corresponding respectively to diagonal and off-diagonal matrix elements of $\hat{H}$. The parameters that define this model are obtained by a least-squares fit that minimizes differences between observed and calculated energies and relative intensities. Alternatively, some of these parameters may be obtained from *ab initio* potentials or by transfer from similar molecules.

Time Domain. The ZOBS has a fast (envelope) decay rate and a countable number of quantum beat features, each with its own frequency, amplitude, phase, and decay rate. There is a simple Fourier transform relationship (i.e., a generalization of eqs 2.8−2.15 for multiple states) between the information in time- and frequency-domain experiments. However, there are often technical reasons that make one kind of experiment easier than another to perform or analyze. For example, a high-resolution spectrum can take a long time to record, and the relative intensities of widely separated features can be ill determined. Conversely, the dynamic range of intensities in a time-domain experiment can be insufficient to resolve a large number of low-amplitude quantum beats. (Note that the number of features in an N-line spectrum scales simply as N, whereas coherent excitation produces $N(N-1)/2$ quantum beats in the time domain.) However, the information in a time-domain spectrum can be simplified and systematically examined by restricting the frequency region of the detected fluorescence or by exploiting phase coherent pump−probe schemes in which the frequency, time delay, and optical phase of the probe pulse are all specified.[140,141]

With this as background, we now turn to a series of examples of IVR studies that attempt to elucidate the key dynamics occurring in each of three qualitatively different energy regimes on the potential energy surface.

III. Low-Energy Vibrational Excitation: IR Fluorescence and Direct Absorption Studies

A. Background. A natural starting point in a discussion of IVR is near the *bottom* of the potential well, where in the absence of fortuitous resonances between zero-order modes the energy level patterns of the zero-order bright states can be well described by harmonic and low-order anharmonic terms. However, the lack of strong coupling with other modes does not mean that IVR phenomena are not of crucial importance in this regime. Specifically, the density of near-resonant dark or bath states, ρ, grows rapidly with molecular complexity and even at fundamental excitation energies can exceed many hundreds of states per cm^{-1}. Thus, significant mixing of the ZOBS with dark states can occur for average or rms coupling matrix elements as small as $1/\rho_{\text{bath}}$, which, when viewed with sufficient spectral resolution, leads to "fractionation" of the single ZOBS transition into spectral clumps of closely spaced lines with effective width $\Delta\omega$ and mean density ρ. As a result of recent advances in high-resolution IR laser spectroscopic methods in jet-cooled beams, this IVR fractionation has been mapped out for several homologous series of molecules with exquisite sensitivity and detail in the frequency domain, which will be discussed later in this section. This unraveling at high resolution of the so-called true molecular eigenstates is the spectral "signature" of IVR in the frequency domain.

Of course, this IVR signature due to fractionation of the ZOBS is also apparent in the time domain. For example, *coherent* excitation of the entire clump of N lines by definition generates the ZOBS, which will evolve according to eq 2.13, suitably generalized for multiple-state mixing. After an initial period (which we may use to characterize an IVR lifetime from $\tau_{\text{IVR}} = 1/\Gamma$), there will be extensive cancellation of the coherent time-dependent terms (with extremely long recurrence times). The square modulus of the autocorrelation will therefore be dominated by the long time average of all N molecular eigenstates, which for equivalently coupled dark states would exhibit roughly $1/N^2$ of the original bright state character. For example, if the zero-order state were a CH-stretch excitation near 3000 cm^{-1}, the time-resolved CH-stretch IR fluorescence from all N upper states would decay (in roughly $1/\Gamma$) to $N \times 1/N^2 = 1/N$ of the initial value, whereas fluorescence at other frequencies from zero-order dark states mixed by IVR would grow in on the same time scale. Of particular relevance, this long time-average behavior is indistinguishable from an initially *incoherent* excitation of the set of molecular eigenstates that comprises the initial ZOBS and thus samples the IVR-induced "dilution" of oscillator strength into the manifold of dark states.

B. IR Fluorescence Studies in CH-Stretch-Excited Hydrocarbons. In a pioneering series of experiments, McDonald and co-workers[2,142−145] tested these ideas using a pulsed IR optical parametric oscillator (OPO) light source to prepare supersonic jet-cooled hydrocarbons in the $v_{\text{CH}} = 1$ levels and monitor the IR fluorescence in the CH stretch and other spectral regions. Since the IR-detector time resolution (>1 μs) was far slower than any anticipated IVR lifetimes, no explicit time dependence was expected. However, by calibrating against known IR absorption strengths, the "dilution factor" ($1/N$) could be used to infer N, the effective number of strongly coupled states. Studies on an extensive set of CH-stretch-excited *fundamentals* indicated a clear inverse correlation of "dilution factor" with density of symmetry-selected rovibrational states; $\rho = 10-100/\text{cm}^{-1}$ was interpreted as the "threshold density"

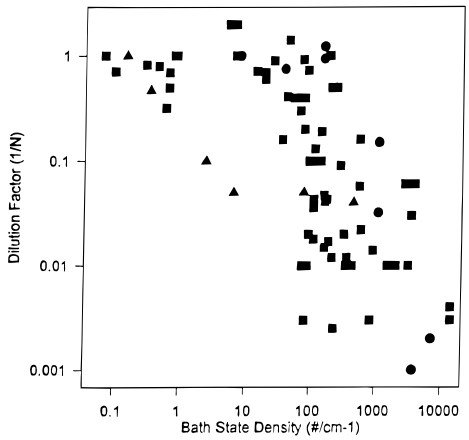

Figure 4. Dilution factor for CH-stretch IR fluorescence subsequent to fundamental ($v_{CH} = 1$) and overtone ($v_{CH} = 2$) excitation, plotted versus the density of vibrational states of appropriate symmetry: circles ($v_{CH} = 1$ aliphatic CH stretches); squares ($v_{CH} = 1$ acetylenic CH stretches); triangles ($v_{CH} = 2$ aliphatic CH stretches). Note the considerable *decrease* in dilution in the vicinity of $\rho = 10-100$ cm^{-1}. Data for $v_{CH} = 1$ and $v_{CH} = 2$ are taken from refs 142 and 146, respectively.

necessary for promoting efficient IVR (see Figure 4). Corresponding IR *overtone* fluorescence studies were also pursued by Nesbitt and Leone[146] for a series of simple alkanes and alkenes in the CH-stretch $v = 2 \leftarrow 0$ region. The results for $v_{CH} = 2$ levels proved consistent with the $v_{CH} = 1$ studies; i.e., the observed $1/N$ dilution factors dropped off rapidly with bath state density above 10−100 states/cm^{-1}. If each of these dark states was equivalently coupled to the bright state, this would imply IVR clump structures *in the threshold region* with coupling matrix elements on the order of $1/\rho$, i.e., $10^{-1}-10^{-2}$ cm^{-1}. This later proved to be in rather remarkable agreement with direct IR laser absorption studies at Doppler and sub-Doppler spectral resolution, although the implicit suggestion that IVR rates would scale in proportion to total state density proved to be untrue. Further efforts by McDonald[144] to look at dilution factors as a function of jet rotational temperature suggested some rotational enhancement (i.e., Coriolis or centrifugal mixing) of the IVR coupling matrix elements, an observation selectively supported by later high-resolution studies.

C. Probing IVR Coupled States: High-Resolution Direct IR Absorption Studies. The indirect influence of such IVR state mixing was certainly noted in the early studies of torsional tunneling splittings in CH stretch excited ethane by Pine and Lafferty.[147] However, direct observation of the IVR-induced clump structures in CH-stretch-excited hydrocarbons was first achieved in a series of high-resolution IR laser measurements by Perry and co-workers[62,63] and McIlroy and Nesbitt.[51−53] The initial system studied was acetylenic CH stretches in species such as 1-butyne and measured via direct absorption of single-mode tunable IR lasers under either pinhole ($\Delta\nu = 200$ MHz) or slit ($\Delta\nu = 30-50$ MHz) supersonic jet conditions. Even higher resolution ($\Delta\nu = 10$ MHz) studies of CH-stretch-excited hydrocarbons exploiting skimmed beams and bolometric detection were later implemented by Lehmann, Scoles, and co-workers.[3,55−61] As expected, each rovibrational transition (i.e., accessing a single ZOBS) in 1-butyne was observed to be split at high resolution into 0.01−0.02 cm^{-1} broad clumps of closely spaced transitions (see Figure 5). These splitting patterns were identical for P/R-branch transitions to the same upper $J_{K_aK_c}$ level and thus unambiguously due to vibrational interactions in the *upper* state. From the set of observed frequencies (N) and relative intensities ($N - 1$), the off-diagonal coupling matrix elements, uncoupled energies of the zero-order "bright" and "dark" basis states, and statistics on the number and density of interacting states could be extracted from a Lawrance and Knight deconvolution procedure.[21] For the interested reader, Lehmann et al.[3] provide an excellent review of these high-resolution IR methods.

The results of these and other high-resolution IR studies on a series of CH-stretch-excited hydrocarbons allow several rigorous tests of different IVR models. For example, splittings in the rotationless ($J' = 0$) upper level are observed, indicating that purely anharmonic state-mixing effects must be important. This is confirmed by analysis of matrix elements (V_{ij}) extracted from a Lawrance and Knight deconvolution,[21] which, for many CH-stretch-excited hydrocarbons, are of order 10^{-2} cm^{-1} and often depend only weakly on the J and K_a states. However, no simple spectral pattern exists between clump structures for successive J values, such as would be predicted for isolated crossings, indicating that the dark states "tune" rapidly through the bright state and are only within the spectral coupling window for at most a few J values. Within experimental uncertainties, the observed densities of the coupled states are equal to the total vibrational state density from harmonic and anharmonic predictions, indicating that IVR appears to couple the ZOBS to the majority of background vibrational states. Most relevant to prospects of vibrational control of chemical reactions, the explicit time-dependent autocorrelation function for these coherently prepared CH-stretch ZOBSs can be obtained directly from the high-resolution frequency-domain data. These data indicate that IVR relaxation occurs only on the 10^{-9} s time scale. This corresponds to more than 10^5 vibrations of the CH group, which is a surprisingly long time when contrasted with picosecond time-scale predictions from earlier thermal and chemical activation studies.[148,149]

D. Structural and/or Density of States Dependence of IVR Rates. These frequency-domain studies of 1-butyne raised a simple but intriguing question: Will these CH-stretch IVR relaxation rates depend on what group is substituted on the other side of the CC triple bond, or is the IVR rate sensitive primarily to the "local" CCH environment? From a simple but common misapplication of Fermi's Golden Rule, one could argue that the IVR rates should *increase* with vibrational state density. On the other hand, drastically increasing total state density by adding modes with vanishingly small coupling to the zero-order bright state also *decreases* the mean square coupling matrix element. Mathematically, ρ_N states/cm^{-1} with a mean square coupling of $\langle V_{ij}^2 \rangle$, diluted by an additional *uncoupled* density of ρ_M states cm^{-1}, leads to a lower mean square coupling strength of $\rho_N \langle V_{ij}^2 \rangle / (\rho_N + \rho_M)$, that is, by exactly the same factor, $(\rho_N + \rho_M)/\rho_N$, by which the density is increased. Thus, if the IVR dynamics is dominated by purely "local" couplings, correct application of Fermi's Golden Rule predicts little or no change in IVR lifetimes in a homologous series with increasing molecular complexity.

This question was initially addressed[52,53] in a high-resolution study by McIlroy and Nesbitt of CH-stretch-excited (i) propyne (R = methyl), (ii) 1-butyne (R = ethyl), and (iii) the *gauche* and *cis* isomers of 1-pentyne (R = propyl), for which the predicted state densities range over 4 orders of magnitude from 0.1 to 2400 states/cm^{-1}. The results (Table 1) indicate IVR lifetimes that are remarkably *insensitive* to the nature of the substitution group, varying by no more than a factor of 2 for more than a 10^2 increase in state density. These terminal acetylene studies have been significantly extended by Lehmann, Scoles, and co-workers[3,57−61] at even higher resolution with bolometric methods, probing systems such as $(CF_3)_3C-CCH$ with state densities as high as 10^{11} states/cm^{-1}! Again, despite an enormous range of 10^7 in state density, the observed IVR

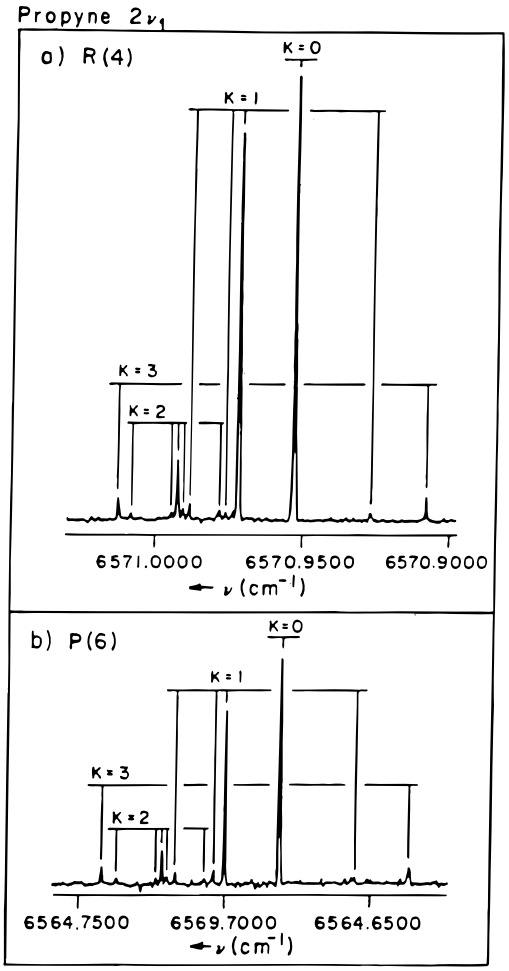

Figure 5. Frequency-domain IVR in the $2\nu_1$ acetylenic CH-stretch excitation of propyne, as evidenced by the additional spectral "clump" structure observed only at high-resolution (0.0005 cm^{-1}) conditions. The precise repetition of the spectral clump patterns in both R(4) and P(6) rotational transitions provides unambiguous evidence that the IVR coupling occurs only in the *excited* (i.e., $J = 5$) state. Note that the $K = 0$ level is unperturbed; this suggests that the IVR mixing is mediated via Coriolis (z-axis, i.e., $\Delta K = 0$) rotational effects, which yield matrix elements proportional to K. Reprinted with permission from ref 55. Copyright 1994 American Institute of Physics.

TABLE 1: IVR Lifetimes[a] for $v_{CH} = 1$ CH-Stretch Excitation in R−C≡C−H Terminal Acetylenes

molecule	τ_{IVR} (ps)	ρ_{bath} (states/cm^{-1})
prop-2-yn-1-ol	500	20
1-butyne	270	22
$(CH_3)C-C\equiv CH$	200	490
1-pentyne (*trans*)	440	2400
1-pentyne (gauche)	240	2400
$(CD_3)_3C-C\equiv CH$	40	2800
$(CF_3)_3C-C\equiv CH$	60	1.0×10^{11}

[a] References 52, 57, 58, and 59.

rates (see Table 1) are within 1 order of magnitude for all acetylenic systems investigated. From the above discussion, it is apparent that the huge reservoir of state density provided by the larger substitution groups has essentially little or no coupling with the zero-order bright CH-stretch state. This is an exceedingly important and simplifying result for efforts to model IVR dynamics theoretically and indicates that state mixing in these systems is rate limited to a highly restricted region of vibrational phase space.

It is worth noting that these high-resolution results would at first appear to be qualitatively different from the results reported by Smalley and co-workers[16−18] in classic low-resolution dispersed fluorescence studies of jet-cooled *n*-alkylbenzenes. These earlier studies took advantage of the negligible shifts in Franck−Condon ring mode progressions with length of the alkyl "tail", which permitted them to systematically vary the density of bath states over many orders of magnitude. The ratio of vibrationally relaxed (broad) to resonance (sharp) fluorescence was observed and used in conjunction with known fluorescence lifetimes to *infer* an *effective* IVR rate from the initially excited ring vibration. Their results clearly demonstrated a dramatic increase of this broad to sharp fluorescence ratio with alkyl chain length and bath state density.

What is the reason for these apparent differences between ring-mode excitation in alkyl-substituted benzenes and terminal CH-stretch excitation in substituted acetylenes? Although it is possible that CH stretches and low-frequency aromatic ring modes exhibit qualitatively different behavior or that complications due to low-lying electronic states may depend on chain tail length, a much simpler explanation exists. Essentially, if the excitation pulses are insufficiently fast to prepare the full ZOBS *coherently*, then the laser instead excites a subset of molecular eigenstates (mostly *incoherently*) whose subsequent fluorescence reflects the long-time behavior corresponding to a "prerelaxed" vibrational distribution of bath levels. Thus, the chain-length-dependent alkylbenzene intensity ratios observed by Smalley would be more analogous to the dilution factors that McDonald measured for IR fluorescence in CH-stretch-excited hydrocarbons,[2,142−145] irrespective of the 10^{-7} vs 10^{-2} s radiative lifetimes of the upper state. Indeed, Parmenter[1] has cleverly exploited the inverse of this point in a series of "chemical timing" experiments, which use high-pressure quenching gases to isolate the fluorescence that occurs exclusively from the ZOBS on the picosecond time scale even for cw laser excitation. High-resolution studies of low-frequency ring vibrational modes in these jet-cooled alkylbenzene systems have not yet been reported but could prove quite interesting to pursue. Indeed, from previous IR studies one might speculate that high-resolution alkylbenzene spectra would reveal IVR clump structure in these ring modes, with clump widths consistent with IVR lifetimes largely *independent* of alkyl tail length and total vibrational state density.

These IVR rates in CH-stretch-excited terminal acetylenes indicate localization of vibrational energy on a surprisingly *long* time scale, considerably longer than the sub-picosecond lifetimes that had previously been inferred from chemical activation studies. As an important benchmark for comparison, this 0.1−1.0 ns localization of the CH-stretch excitation is comparable to typical gas kinetic collision times at 1 atm.[150] In conjunction with the very exciting results on vibrationally enhanced chemistry in small systems (where IVR is not an issue) such as Cl and H atom reactions with H_2O/HOD by Crim and co-workers,[12,13] this bodes well for extension to significantly *larger* molecular systems, where IVR had previously been considered too fast for vibrationally mediated "control" of bimolecular reactions in the gas phase.

E. Double-Resonance State Labeling. The *sine qua non* in these high-resolution studies is to isolate the purely *homogeneous* IVR-induced structure, uncomplicated by the residual *inhomogeneous* structure due to, for example, different $J_{K_aK_c}$ rotational states, isomers, isotopes, etc. With the introduction of IR/microwave/visible double-resonance techniques, high-resolution spectroscopic studies of IVR mode mixing have been refined to new heights of experimental elegance and flexibility. In the double-resonance method of Perry, for example, two independent IR lasers can be both tuned and modulated at different frequencies; if the lasers share any common level

TABLE 2: IVR Lifetimes for $v_{CH} = 1$ and 2 Quanta CH-Stretch Excitation (Experiment[a] and Theory[b])

	$\tau_{IVR}v=1$ (ps)		$\tau_{IVR}v=2$ (ps)	
molecule	exp	theory	exp	theory
$(CH_3)_3C-C\equiv CH$	200	260	110	90
$(CD_3)_3C-C\equiv CH$	40	35	<40	50
$(CH_3)_3Si-C\equiv CH$	2000	$>5.2 \times 10^4$	4000	1300
$(CD_3)_3Si-C\equiv CH$	830	260	140	170
$(CH_3)_3Sn-C\equiv CH$	6000		>1000	

[a] References 57 and 58. [b] Reference 85.

(upper or lower) and one laser is partially saturating the transition, the modulation of the saturating laser will be written onto the transmission of the other. Alternatively, with the EROS (electric resonance optothermal spectroscopy) scheme of Fraser, Pate, and co-workers,[69−71] optical lasers have been combined with classic radio-frequency/microwave electric resonance methods to probe transitions between states via deflection toward or away from a bolometer.

The significance of these double-resonance methods is the achievement of maximal rotational ($J_{K_aK_c}$) state selection and labeling, as well as excitation into even higher *overtone* and *combination* vibrational levels. This overtone capability has permitted Lehmann, Scoles, and co-workers[47−61] to study the dependence of acetylenic CH-stretch IVR rates on the number of vibrational quanta (Table 2). For the terminal CH acetylenic systems investigated thus far, the dependence of IVR lifetimes on v_{CH} is remarkably small, often less than a factor of 2, and in some special cases even *slowing* with increasing quantum number. Even though there are interesting structure and moiety-specific trends to be discovered (discussed in section VI), all spectroscopically measured IVR rates in the acetylenic $v_{CH} =$ 1, 2, and 3 CH-stretch manifold have proven to be (i) surprisingly *slow* ($(20-0.2) \times 10^9$ s^{-1}), (ii) within a relatively "narrow" window (less than 2 orders of magnitude), and (iii) remarkably *insensitive* to total state density. This last point deserves particular emphasis, since a common conclusion from lower-resolution studies has been that total state density is a *key* parameter controlling IVR rates.

F. Probing the Nature of Bath States. This discussion of multiple-resonance methods highlights an important point. From the high-resolution distribution of absorption frequencies and intensities within a spectral clump illustrated by a given ZOBS, one can therefore predict $|\langle\Psi(t)|\Psi(0)\rangle|^2$ *without any further knowledge of the nature of the molecular eigenstates*! This sounds like good news, but the corresponding disadvantage is that even though you know how *fast* the energy leaves the original ZOBS, you do not know where or how fast the vibrational energy subsequently flows! This situation changes qualitatively for multiple-resonance methods, which can independently interrogate other spectral properties of the molecular eigenstates. Stated simply, double-resonance capabilities allow a glimpse of the *eigenfunction* composition of an IVR feature state by projecting it onto a different ZOBS with a second photon. This is, of course, true of any two-color pump−probe experiment, in either time or frequency domain. For example, in the $v_{CH} = 1$ IR fluorescence studies of McDonald and co-workers,[2,142−145] the CH-stretch ZOBS gets to "choose" at what characteristic frequencies (e.g., CH stretch, CH bend, etc.) to reemit the initial laser excitation. Thus, the dispersed IR fluorescence spectrum can elucidate the nature (after an initial transient) of the bath states that are coupled with the zero-order bright state.

In order to sample the character of the excited-state eigenfunctions, this second probe field need not be provided by another photon. A beautiful example of this has been reported by Fraser et al.,[69−71] who measured the electric field-induced Stark shifts of IVR mixed energy levels in OH-stretch-excited ethanol. In the absence of any IVR state mixing, one would anticipate a strong dipole moment for the OH-stretch-excited state. Thus, a coherently prepared ZOBS should tune rapidly with E-field, and therefore it should be possible to deflect molecules by a force proportional to the electric field gradient. Specifically, all eigenstates can be separated into those that focus or defocus in a quadrupole field, and thus resonances are detected when a transition converts a molecule from a focusing to a defocusing state. Indeed, such Stark-induced forces are precisely what makes the EROS method work for many other molecular applications. What Fraser et al. observe, however, is the complete *lack of any* measurable deflection for strongly IVR-mixed levels in the OH-stretching state; the individual eigenstates in vibrationally OH-stretch-excited ethanol exhibit no apparent dipole moment, even though the coherently prepared ZOBS certainly must.[70,71]

The resolution of this apparent paradox provides important insights into IVR phenomena. There is a dense manifold of energy-level-avoided crossings as the molecular eigenstates attempt to tune in the E-field. Due to off-diagonal terms in the Hamiltonian, however, the levels do not actually cross, but instead the dominant zero-order character switches as the field tunes the eigenstates through the crossing region. Due to this dense "traffic jam" of avoided crossings, no individual eigenstate succeeds in tuning *very far* in energy, even though a coherently excited ZOBS would exhibit a clear second-order Stark shift. Consequently, the *average* slope of energy versus E-field for the eigenstates vanishes and thus the molecules are not deflected by the external E-field gradient.

IV. Intermediate Vibrational Excitation on the Potential Surface: High-Overtone Studies of IVR

A. IVR in CH-Stretch-Excited Benzene Overtones: Role of Nonlinear Resonances. Even though arguably the most detailed spectroscopic information on IVR phenomena near the potential surface minimum has been obtained via the high-resolution methods described above, the associated excitation energies in those studies are typically only a small fraction ($\lesssim$10%) of a typical covalent chemical bond strength. Consequently, there has been considerable interest in developing a similarly detailed understanding of IVR dynamics at "chemically significant" energies, accessing regions of the potential surface where large-amplitude, anharmonic coupling effects begin to be quite dramatic and which may even sample high-barrier, unimolecular chemical transformations such as isomerization. One approach to this energy regime, pursued by several groups, has been high-overtone excitation of high-frequency stretching modes,[32−50] with particular emphasis on near-IR/visible/UV overtone absorption spectroscopy in the CH-stretch manifold.

Of the numerous studies of CH-stretch-excited hydrocarbons, there has been a special focus on the benzene molecule, which has historically been the "hydrogen atom" of high-overtone spectroscopic studies of IVR. This was stimulated by the development of sensitive intracavity dye laser photoacoustic methods, which Berry, Bray, and Hall[49,50] used in pioneering studies to measure CH/CD-stretch-overtone spectra in room temperature benzene vapor up to as high as $v_{CH} = 9 \leftarrow 0$. Although the initial interpretations of the data were somewhat flawed, these studies raised some very important questions about IVR in CH-stretch-excited hydrocarbons and in turn stimulated an enormous amount of subsequent theoretical and experimental effort.

Specifically, the benzene spectra reveal a clear CH-stretch-overtone progression, with a Birge−Sponer anharmonicity analysis characteristic of localized CH-stretch excitation. Furthermore, despite the fact that the low-overtone spectra contain significant contributions from inhomogeneous broadening at room temperature, the spectroscopically observed line widths for the higher overtones are quite broad (30−110 cm^{-1}), which was interpreted to imply rapid IVR on the subpicosecond time scale. However, these line widths depend in a surprisingly *nonmonotonic* way on the number of vibrational quanta excited, *increasing* for $v_{CH} = 4 \leftarrow 0$ to $v_{CH} = 7 \leftarrow 0$ and then eventually *decreasing* for $v_{CH} = 8 \leftarrow 0$ and $v_{CH} = 9 \leftarrow 0$. Furthermore, this nonmonotonic trend is sensitive to H/D isotopic substitution, suggesting the presence of low-order vibrational resonances between CH/CD stretches and other modes in benzene. As interpreted in elegant detail by Sibert et al.,[86−88] these theoretical studies identified the source of IVR line width as a nonlinear 2:1 Fermi resonance between the CH-stretch and CCH-"bend" manifolds. This vibrational state mixing tunes in and out of resonance due to the anharmonicity of the CH stretch. The remarkable success of this analysis is that experimentally observed IVR line widths in a complicated molecule, as well as the isotopic dependence thereof, could be qualitatively reproduced from relatively simple model calculations on a trial force field. A particularly important result of this study is that the time scale for fast IVR dynamics in benzene could be predicted by analysis of *local* stretch−bend interactions on the same functional group. It is precisely this sort of *moiety-specific* description of IVR, developed from detailed analysis of a finite number of test molecules, that would ideally permit extrapolation of IVR time scales, tier structures, and energy flow paths to more general molecular systems.

B. Stretch:Bend Fermi Resonances in Isolated CH-Stretch Chromophores. The relevance of such 2:1 stretch:bend Fermi resonances in CH overtone spectra has been beautifully elucidated in a series of studies by Quack and co-workers[41−45] of substituted methanes such as CHX_3 (X= D, F, Cl, Br, CF_3). Specifically, by making the CH stretch chemically unique, they were able to study the stretch−bend coupling in isolation. As a result of this 2:1 Fermi resonance (i.e., $v_{bend} \approx 1500$ cm^{-1}, $v_{stretch} \approx 3000$ cm^{-1}), there exists a set of *near*-resonant stretch−bend states in the vicinity of the ZOBS that satisfies the expression

$$N = v_{stretch} + 0.5v_{bend} \tag{4.1}$$

and forms a vibrational polyad of order $N + 1$. By applying the scaling rules of section II.C and eq 2.6, the associated tier structure becomes quite simple; the ZOBS is $|v_{stretch},0\rangle$, the first tier consists exclusively of $|v_{stretch} - 1,2\rangle$, the second tier, $|v_{stretch} - 2,4\rangle$, etc. The Hamiltonian matrix is therefore block diagonal, with adjacent off-diagonal elements determined analytically by cubic terms (i.e., $Q_{stretch}Q_{bend}^2$) in the potential. Due to the sequential nature of the coupling, the bright state character of the overtone is mixed into each of the $N + 1$ molecular eigenstates, but with a magnitude that drops rapidly with decreasing overtone character. Results for the second overtone spectrum ($N = 3$ polyad) of HCF_3 are displayed in Figure 6, which shows the anticipated cluster of $N + 1 = 4$ bands of monotonically decreasing intensity. From analysis of the series of polyad overtone spectra, both the intensity patterns and vibrational band origins can be quantitatively fit to low-order quadratic and cubic terms in the potential.

Due to a combination of strong coupling and detuning of these zero-order stretch−bend vibrations, the spacing of the resulting

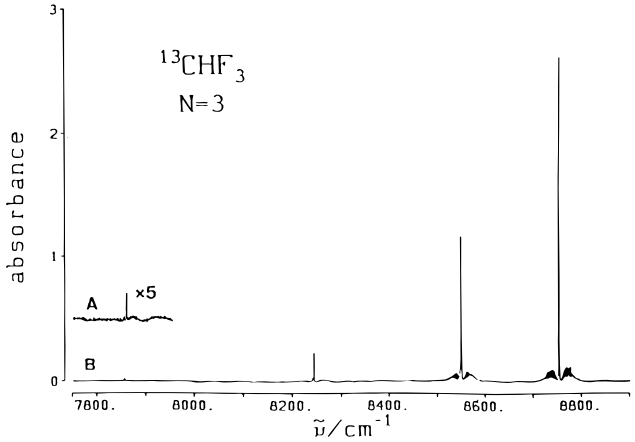

Figure 6. Moderate-resolution FTIR $N = 3$ overtone polyad of the CH stretch in $^{13}CHF_3$. Note the clear evidence of $N + 1 = 4$ CH-stretch bands, due to successive mixing of the initial ZOBS (i.e., $|v_{stretch},v_{bend}\rangle = |3,0\rangle$) with near-resonant $|2,2\rangle$, $|1,4\rangle$, and $|0,6\rangle$ tiers via 2:1 Fermi resonant bend−stretch coupling. The relative intensities and shifts provide quantitative support for such a near-resonant tier model. Reprinted with permission from ref 43. Copyright 1985 American Institute of Physics.

molecular eigenstates is now so large (≈1000 cm^{-1}) that it would require extremely fast IR pulses (≲15 fs) to prepare the original ZOBS coherently. In principle, however, such a coherent excitation would lead to sequential IVR flow of the initial ZOBS overtone state $|v_{stretch},0\rangle$ into the dark states with $|v_{stretch}-1,2\rangle$, $|v_{stretch}-2,4\rangle$, etc., on a time scale given by a multistate generalization of eq 2.14. However, due to the multiple tier level participation in the IVR mixing, population transfer is by no means as simple or complete as in a two-level system. For example, in this simple case of IVR with only four coupled states, there would be partial recurrences in the autocorrelation function characteristic of "quantum beats". There would also be much smaller amplitude recurrences in the cross-correlation or "probability transfer" functions corresponding to each of the dark states in the polyad.[44,45] This is analogous to the quantum beat time-domain structures observed in electronically excited state fluorescence studies by Felker, Zewail, Field, Zare, and others[22−26,110,111] and has been characterized as "restricted IVR" due to the relatively small number of strongly coupled bright and dark states. This example also nicely stresses the utility of the IVR tier structure concept, whereby a polyad pattern of sequential mode couplings takes on a physical reality as a sequential flow of vibrational energy, with a nested sequence of time scales and decreasing amplitudes. Similar tier analyses of more complicated multiple Fermi resonance behavior in systems such as NH_3[151,152] and HCCF[153,154] have also been successfully performed.

C. CH-Stretch Overtones in Jet-Cooled Benzene: Comparison of Theory and Experiment. Based on the above discussion, high-resolution overtone spectra of benzene might be anticipated to reveal additional structure corresponding to CH stretch−bend Fermi resonance mixing, in addition to even finer structures that would identify the IVR relaxation pathways relevant at even longer time scales. However, this is not observable in the room temperature benzene photoacoustic spectra, due to inhomogeneous broadening from rotational band contours and sequence congestion from low-frequency vibrational hot bands. In order to eliminate such thermal effects, these benzene overtone experiments have been performed under supersonic jet conditions by (i) Page et al. using IR + UV double-resonance methods[155] and (ii) Scotoni et al. using optothermal bolometric methods.[156] The results from both groups indicate considerable narrowing of the $v_{CH} = 3 \leftarrow 0$

overtone spectrum with supersonic rotational cooling, revealing a rich, albeit complicated, spectral substructure with features as narrow as 5 cm^{-1} and clearly showing that the photoacoustic line widths for the lower v_{CH} levels are substantially broader than the homogeneous width. Though the size of benzene makes this quite challenging, considerable progress toward an interpretation of this spectral structure has been made by Wyatt and co-workers[93−97] and Marcus and co-workers.[157,158] These quantum vibrational calculations require including many more degrees of freedom than in the Sibert et al. study[86−88] and are computationally extremely intensive. Though all 30 degrees of freedom in benzene cannot yet be treated, converged results have been obtained that include all 21 in-plane vibrational modes.[93−97] Nevertheless, semiquantitative agreement has been achieved between experiment and theoretical predictions, in terms of both line widths and detailed spectral structure. The calculations also directly confirm the central importance of CH stretch−bend Fermi resonances in the early time IVR processes.

D. Vibrationally Mediated Photolysis. As noted in section II, any sufficiently high-resolution one-photon absorption spectrum can predict completely the magnitude of the time-dependent autocorrelation of $\Psi(t)$ with the original ZOBS, i.e., $\Psi(0)$. However, it tells us frustratingly little about *where* the energy eventually goes, i.e., what comprises the dark state manifold. Although in principle one can glean this information from dispersing the IR *emission* spectra of the resulting molecular eigenstates, an even more useful strategy has been to probe the resulting *absorption* spectra. This has been attempted for low CH-stretch levels ($v_{CH} = 2$) via high-resolution double-resonance studies ($v_{CH} = 2 \leftarrow 1$, $1 \leftarrow 0$) in terminal acetylenes by Perry and co-workers[66,67] and Lehmann and co-workers.[60,61] Though at considerably reduced resolution, a very useful alternative method has been pursued by Rizzo and co-workers[32−36] in a classic series of studies of OH-stretch-excited species. This method takes advantage of vibrationally mediated photodissociation schemes of Crim and Andresen to prepare a molecule above the dissociation threshold to generate OH, followed by LIF detection of the radical. For example, a pulsed dye laser is used to excite the $v_{OH} = 4 \leftarrow 0$ overtone region in nitric acid (HNO_3), which lies just below the energetic threshold, to form OH + NO_2 fragments. Since any further excitation of OH-stretch vibrational quanta energetically leads to predissociative formation of OH radicals, a second IR pulsed laser can then "map" out the resulting absorption/action spectrum of the $v_{OH} = 4$ overtone-excited nitric acid molecules. The large anharmonicity for OH-stretch excitation in nitric acid allows the effective vibrational quantum number to be estimated from the center frequencies of features in the absorption profiles. Specifically, if there is only weak IVR mixing of high OH-stretch overtones with the bath, the $\Delta v = +1$ absorption spectrum for the second laser would resemble that of a single $v_{OH} = 5 \leftarrow 4$ band, whereas in the limit of strong mixing, the corresponding $\Delta v = +1$ spectrum would be sequentially blue-shifted by OH-stretch anharmonicity into the $v_{OH} = 4 \leftarrow 3$, $3 \leftarrow 2$, $2 \leftarrow 1$, $1 \leftarrow 0$ regions. Indeed, the absorption/action spectrum for the second laser reveals precisely such a sequence of bands, the relative intensities of which correspond well to the predicted *total* densities of vibrational states for a given v_{OH} at the total vibrational energy of the initial excitation (see Figure 7). Thus, the results indicate essentially *complete* mixing of all vibrational states of nitric acid in the $v_{OH} = 4$ and $v_{OH} = 5$ regions. This is consistent with both the earlier IR fluorescence studies of $v_{CH} = 1$ and 2 stretch excited hydrocarbons and the dark state densities inferred from high-resolution IR laser absorption studies of terminal acetylenes.

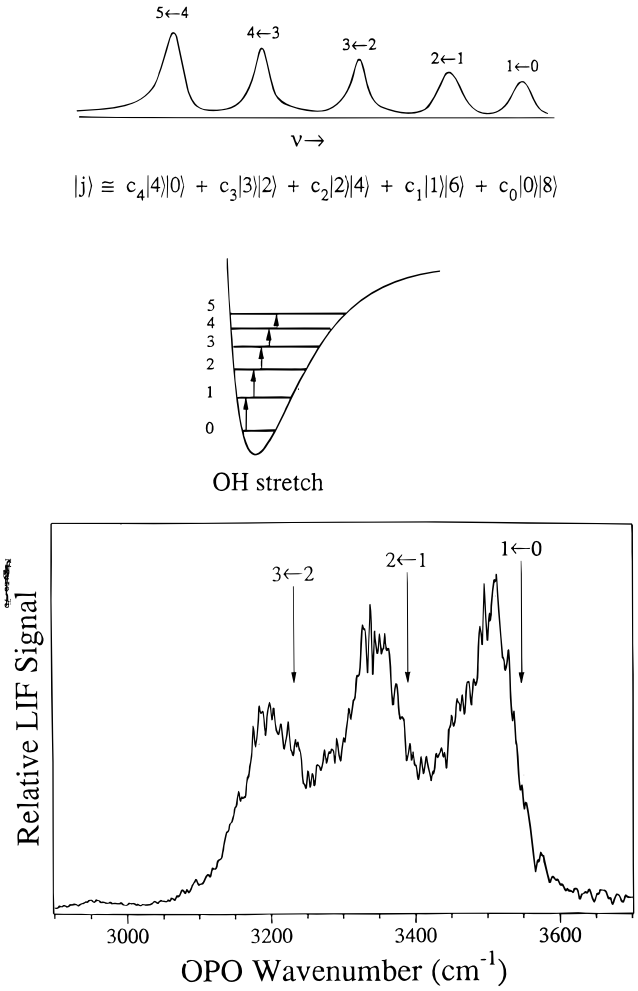

Figure 7. An IR double-resonance $\Delta v = +1$ absorption spectrum of HNO_3 originating from the $v_{OH} = 4$ level. The arrows identify the origins of the various $\Delta v = +1$ bands. If this upper state were completely free of IVR mixing, the subsequent $\Delta v = +1$ IR absorption would occur at the substantially red-shifted $v_{OH} = 5 \leftarrow 4$ region. Instead, absorption bands clearly corresponding to $v_{OH} = 3 \leftarrow 2$, $2 \leftarrow 1$, and $1 \leftarrow 0$ are observed. A quantitative analysis of these band intensities is consistent with a statistically mixed nature of the $v_{OH} = 4$ level into near-resonant bath states. Reprinted with permission from ref 35. Copyright 1991 American Institute of Physics.

E. Franck−Condon Pumping/SEP Studies of Acetylene. Thus far in the discussion, there has been a clear emphasis on high-overtone studies involving CH-, OH-, or NH-stretch excitations. This is due both to the relatively large quantum of vibration (~3000 cm^{-1}) and to the unusually large mechanical and electronic anharmonicity of hydride-stretching motions, which makes overtone excitation at chemically significant energies possible. With Franck−Condon pumping/SEP schemes as an alternative, however, a much broader range of vibrational levels can be accessed in favorable molecules. One system that has received extensive attention with SEP methods is acetylene. This is arguably the *simplest* possible molecule in which all features relevant to vibrational dynamics in larger polyatomics are qualitatively represented and therefore provides an excellent pedagogical example of what analysis of IVR can hope to achieve.

The special characteristic of acetylene that makes this possible is that its vibrational density of states grows relatively *slowly* with energy; thus, fully resolved spectra can be recorded up to chemically interesting levels of vibrational excitation, $E_{VIB} \leq 20\,000$ $cm^{-1} = 57$ kcal/mol, which is well above the barrier to a bond-breaking isomerization between acetylene and

vinylidene.

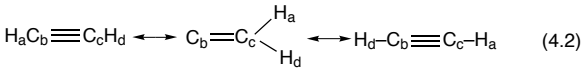

(4.2)

As demonstrated below, this SEP access to a wide range of electronic ground state vibrations permits (i) characterization of all resonances that control IVR at low E_{VIB}, (ii) a test of scaling predictions as E_{VIB} is increased systematically along families of ZOBSs, (iii) the development of statistical procedures for extracting structural and dynamical information from incompletely assigned spectra, and (iv) the use of the breakdown of scaling predictions as a pattern-recognition scheme for characterizing chemically important topographic features of the potential energy surface.

1. Characterization of Resonances at Low E_{VIB}. Ever since the first high-resolution infrared and Raman spectra of acetylene were recorded, it was clear that most of the lowest-lying vibrational levels exhibited spectroscopic perturbations (i.e., level shifts, extra lines, anomalous molecular constants) due to several different anharmonic resonance terms in the $V(\mathbf{Q})$. Among these are a 2:2 stretch Darling−Dennison, a 2:2 bend Darling−Dennison, and several 1:1+1+1 quartic interactions where one quantum of a CH stretch (v_1'' or v_3'') is exchanged for one quantum of the CC stretch (v_2'') plus two quanta of the bends (*trans*-bend v_4''; *cis*-bend v_5''). Each of these low-order vibrational resonances can be investigated at *low* E_{VIB} by high-resolution IR, Raman, or SEP spectroscopies and characterized by an effective Hamiltonian matrix (i.e., $\hat{H}^{eff}$) in a product basis of zero-order vibrational states. The vibrational resonance appears in $\hat{H}^{eff}$ as off-diagonal matrix elements, each expressed as a coupling strength (one for each resonance) times an *a priori* known function of normal mode quantum numbers (e.g., eq 2.6). The simplified matrix elements of $\hat{H}^{eff}$ are therefore based on harmonic oscillator selection ($\hat{Q}_i^n \rightarrow \Delta v_i = n$) and coupling matrix element scaling rules (e.g., $\hat{Q}_i^n \rightarrow v_i^{n/2}$), with a small number of resonance coupling strengths that have been least-squares fit to match energy eigenvalues and intensities with experiment at low E_{VIB}. Thus, the model $\hat{H}^{eff}$ matrix is large and may appear to be complicated, but each resonance is represented by only one coupling strength parameter.

2. Block Diagonalization of $\hat{H}^{eff}$: Polyads and Polyad Quantum Numbers. As a linear four-atom molecule, acetylene has seven vibrational quantum numbers (v_1, v_2, v_3, v_4, l_4, v_5, l_5), where l_4 and l_5 reflect the vibrational angular momenta associated with the doubly degenerate v_4 and v_5 bending modes. Naively, one might expect that each resonance would destroy at least one vibrational quantum number. Since more than seven strong resonances are known in HCCH, one might expect that there would be no useful (i.e., approximately good) quantum number labels for the molecular eigenstates. This would be bad news for characterizing IVR mechanisms in acetylene, because assigning quantum number names to eigenstates or feature states is the first step in determining "where" (as opposed merely to "how fast") the energy flows.

But condolences are premature! These resonances are not all linearly independent. This can be seen by representing each resonance by a 7-D vector in quantum number space, where the components express the harmonic oscillator selection rule for nonzero off-diagonal matrix elements. For example, the stretch Darling−Dennison, $k_{1133}\hat{Q}_1^2\hat{Q}_3^2$, and the "3,245" resonance, $k_{3,245}\hat{Q}_3\hat{Q}_2\hat{Q}_4\hat{Q}_5$, correspond respectively to resonance vectors $(\Delta v_1,\Delta v_2,\Delta v_3,\Delta v_4,\Delta l_4,\Delta v_5,\Delta l_5) = (2,0,-2,0,0,0,0)$ and $(0,1,-1,1,0,1,0)$. By representing each important resonance by a vector in quantum number space, it then becomes a standard problem in linear algebra to find a set of mutually orthogonal vectors that are also orthogonal to *all* of the resonance vectors. Physically, these vectors represent the generalized vibrational quantum numbers that are *not destroyed* by the set of known resonances.

In the case of HCCH, the surviving quantum numbers are

$$n_{res} = 5v_1 + 3v_2 + 5v_3 + v_4 + v_5 \tag{4.3a}$$

$$n_s = v_1 + v_2 + v_3 \tag{4.3b}$$

$$l = l_4 + l_5 \tag{4.3c}$$

In the above expression for n_{res}, the integers can be traced to the approximate 5:3:5:1:1 ratios of the normal-mode frequencies, with $E_{VIB} \approx n_{res}\cdot(650\ cm^{-1})$. Similarly, n_s reflects the total number of quanta in stretching vibrations, and l is the total vibrational angular momentum. These three (approximately) conserved quantities $[n_{res}, n_s, l]$ serve to (approximately) block diagonalize $\hat{H}^{eff}$. Each block of $\hat{H}^{eff}$ is called a polyad and is labeled by the three polyad quantum numbers $[n_{res}, n_s, l]$.

3. Dispersed-Fluorescence Spectra: Scaling of Early Time IVR. The resonances characterized by a least-squares analysis of the low-E_{VIB} levels of acetylene certainly include all of the strongest and most important anharmonic interactions. However, there are, of course, weaker resonances neglected in this treatment that will partially degrade the polyad quantum numbers, in essence by introducing off-diagonal matrix elements between members of different polyads. Thus, IVR in the time domain will consist of relatively fast, *well understood intrapolyad* dynamics plus slower, *mechanistically less well characterized interpolyad* dynamics. This description is intimately related to the concept of IVR tiers, but where we ignore, i.e., truncate, the tier structure beyond a certain limit. By Fourier transforms, we can use this ignorance of the IVR dynamics beyond some time limit to particularly clever advantage. Specifically, if we observe spectra in the high-E_{VIB} region at *reduced* spectral resolution, the data contain information only about the *early time* dynamics, which corresponds to *intrapolyad* vibrational energy flow from a preselected ZOBS. Since it is only this early time behavior that we seek to characterize (at least at first!), dispersed fluorescence (DF) methods at $\sim$5 cm^{-1} resolution with only one excitation laser provide an experimentally much more convenient way of obtaining this information than via SEP methods at $\sim$0.05 cm^{-1} resolution, which require multiple PUMP and DUMP lasers.

Acetylene offers some special advantages that make our job easier; by an accidental combination of Franck−Condon activity and resonance structure, each acetylene $[n_{res}, n_s, l]$ polyad fortuitously contains only one ZOBS! Therefore, by observing dispersed fluorescence from different intermediate vibrational levels in the $\tilde{A}$-state, one can systematically change the relative Franck−Condon intensities of different polyads (e.g., by changing the number of quanta in the $\tilde{A}$-state *trans*-bend), which allows spectrally overlapping polyads to be "unzipped" from each other. Alternatively, one can illuminate a different bright state in each polyad, e.g., by IR−UV double-resonance excitation of an $\tilde{A}$-state vibrational level that is a Franck−Condon dark mode, such as a C−H stretch, a torsion, or an antisymmetric in-plane bend. This second trick allows systematic sampling of the short-time IVR dynamics as a function of additional quanta away from the usual Franck−Condon-allowed ZOBS, which permits one to probe new members of the polyad that may be more strongly coupled to, for example, the unimolecular isomerization path between acetylene and vinylidene.

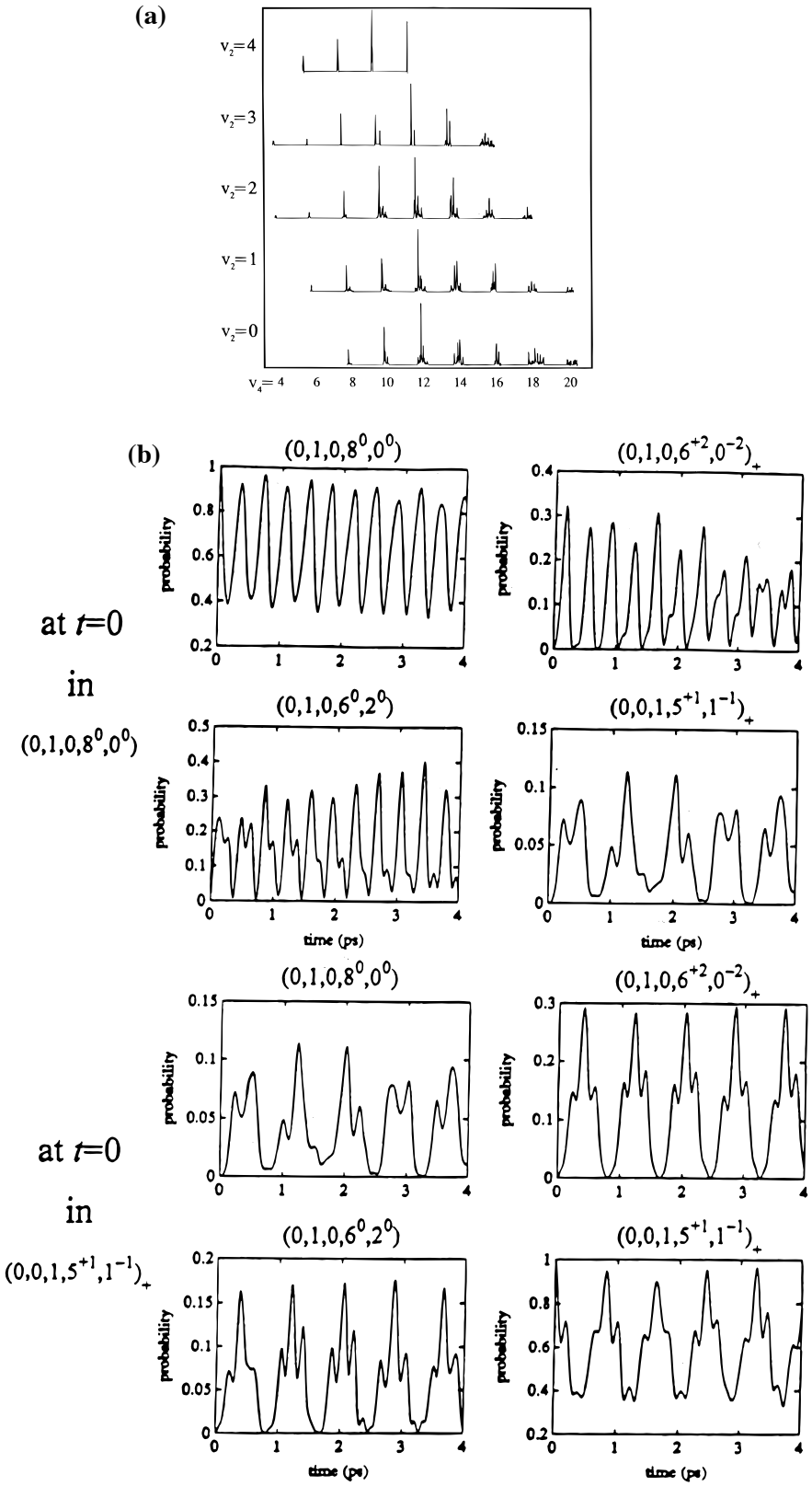

Figure 8. IVR sampled by dispersed fluoresence (DF) spectra of acetylene. By recording DF spectra that originate from two different upper−intermediate levels, overlapping features can be "unzipped" from each other. (a, top) Unzipped spectra, shown as progressions in even quanta of *trans*-bend (v_4'') at constant CC stretch (v_2''). The width and number of resolved subfeatures in each unzipped clump provide sensitive tests of a scalable polyad model for IVR. In this system, IVR (i.e., spectral fragmentation) clearly increases more rapidly with increasing v_2''. (b, bottom) Intrapolyad dynamics in state space resulting from $t = 0$ excitation of a bright state, B, within the $(n_s, n_{res}, l) = (1,11,0)$ polyad. The four panels describe the dynamics when B = $(0,1,0,8^0,0^0)^0$, the initial Franck−Condon ZOBS in the polyad. The upper left shows the "survival probability" (square modulus of the autocorrelation function) of the ZOBS, whereas the other three panels show time-dependent probability of transfer to *first* tier $[(0,1,0,6^{+2},2^{-2})$ and $(0,1,0,6^0,2)^0]$ and *second* tier $[(0,0,5^{+1},2^{-1})^0]$ levels. Reprinted with permission from ref 77. Copyright 1995 VCH.

By way of example, Figure 8a shows the result of such an "unzipping" procedure in the DF spectra of acetylene. Each *row* contains a progression of polyads (E_{VIB} increases left to right) accessed via consecutive excitation in the *trans*-bend (v_4'')

for a constant number of quanta in C−C stretch (v_2''). Each *column* shows a progression of polyads (E_{VIB} increases bottom to top) accessed via consecutive excitation in the C−C stretch, for constant excitation of the *trans*-bend. The plot clearly shows that spectral fractionation symptomatic of IVR *increases* monotonically as excitation in the *trans*-bend *increases*, but *decreases* as excitation in the C−C stretches *increases*! Remarkably, these initially nonintuitive trends in IVR rates can be completely explained in terms of the simple scaling relationships for the coupling matrix elements, energy differences in the zero-order states, and a single (least-squares-fitted) parameter for each low-order resonance. From the time-frequency Fourier transform, the polyad model not only successfully accounts for v_2'',v_4''-dependent trends in IVR fractionation but also explicitly predicts the intrapolyad vibrational energy flow subsequent to excitation of any ZOBS. For example, Figure 8b demonstrates the time-dependent probability of finding the system in each of four different zero-order states following coherent preparation of a specific ZOBS {i.e., $(0,1,0,8^0,0^0)^0$} at $t = 0$.

The frequency- and time-domain patterns presented respectively in Figure 8a,b *appear complicated*, but they are in fact well predicted from a *small* number of well determined spectroscopic (ω_i, x_{ij}) and anharmonic resonance (k_{ijkl}) parameters. The polyad model is the basis for a powerful pattern-recognition scheme that may prove useful in systematically refining *ab initio* surfaces against experimental data or detecting the abrupt change of resonance structure that occurs near chemically important topographic features of a potential energy surface.

V. IVR at "High" Energies: Vibrational Dynamics above Potential Barriers to Unimolecular Bond Breaking and/or Molecular Rearrangement

The analysis of the acetylene spectra described in the previous section provides a clear example of the power of SEP and DF methods for selecting a specific ZOBS, as well as the spectroscopic tools for decoding the IVR dynamics encoded in such a vibrationally energized initial state. An even richer set of dynamical IVR phenomena becomes experimentally accessible when the initial vibrational excitation lies at an energy *above* the ground state barrier to dissociation. In this regime, coupling of the zero-order dark states to the translational continuum can also be important, which introduces an additional "clock," that of dissociation (or predissociation), into the IVR analysis. The time scale for dissociation vs the initial IVR loss of coherence of the ZOBS, for example, can control whether the bond-breaking process is "direct" (ZOBS → fragments) or "sequential" (ZOBS → relaxed distribution → fragments). Furthermore, for polyatomic molecules, there can be significant mode specificity in both the dissociation rates as well as IVR, which can lead to a dependence of the actual dissociation mechanism on the choice of ZOBS.

A. Direct Mode-Specific Photofragmentation. A particularly instructive polyatomic system for detailed investigation of these mixed IVR/dissociation phenomena is HFCO. Specifically, HFCO → HF + CO dissociation rates have been measured by Choi and Moore[79−82] from highly excited vibrational levels of the $\tilde{X}^1A'$ electronic ground state, using a variety of fluorescence-dip-detected SEP-related techniques that exploit vibrational levels of the $\tilde{A}^1A''$ excited state as intermediates (see Figure 9). Similar to the case in the well-studied H_2CO → H_2 + CO system,[31] there is a large barrier (∼17 200 cm^{-1}) to nearly thermoneutral HFCO → HF + CO dissociation on the S_0 surface. Dispersed fluorescence spectra of HFCO include long progressions extending to $E_{VIB} \approx 22\,000$ cm^{-1} in the two Franck−Condon-active modes, ν_2 (CO stretch) and ν_6 (out-of-plane bend). Thus, SEP permits double-resonance access to regions of vibrational phase space on the ground electronic manifold both *below* and *above* the barrier to dissociation, with both ZOBS and rotational ($J_{K_aK_c}$) initial state selectivity.

Three types of SEP experiments have been performed: (i) moderately high-resolution (0.05 cm^{-1}) SEP, which determines the S_0 rotation−vibration energy levels, and dissociation rates from spectroscopic line widths for the states which dissociate fast enough; (ii) SEP−delay−LIF, a PUMP−DUMP−PROBE scheme which measures the lifetimes of HFCO rotation−vibration levels that are too long-lived to broaden the SEP lines beyond the 0.05 cm^{-1} resolution limit; and (iii) SEP photofragment fluorescence excitation based spectral measurement of the vibration, rotation, and translational distributions of the CO photofragments.

The SEP studies of HFCO sample rotation−vibration levels in the $13\,000 < E_{VIB} < 23\,000$ cm^{-1} region. Near 18 000 cm^{-1}, broad spectral clump features in the SEP spectra are observed, corresponding to a dark state density >10 per cm^{-1} for *J*-resolved features. This is more than 5 times the calculated symmetry-sorted vibrational density of states, indicating that extensive IVR coupling essentially to all vibrational dark states is occurring and Coriolis mixing among all (same parity) K_a, K_c states for a given *J* is likely. For lower energies, $E_{VIB} \leq 18\,000$ cm^{-1}, these broad clump features split into many well-resolved peaks, each corresponding to a dissociation-broadened molecular eigenstate. The width and number of components in each clump are found to be strongly dependent on the ZOBS (i.e., v_2, v_6) label for the initial state. For example, the extent of IVR state mixing depends strongly on the number of quanta of ν_6 (the out-of-plane bend), monotonically increasing from essentially no mixing for a pure overtone of ν_6 (e.g., the 6_{19} level at $E_{VIB} = 18\,224$ cm^{-1}) to at least five strongly coupled dark states for the nearly isoenergetic combination level (e.g., the $2_3 6_{13}$ level at 17 823 cm^{-1}).

The most striking observation, however, is the 100 times longer dissociation lifetimes for *pure overtones* of the out-of-plane vibration, which again raises the issue of special stability of states with "extreme" as opposed to more "distributed" vibrational excitations. In the case of HFCO, there is a plausible physical mechanism for such an effect: the minimum-energy dissociation path is in-plane, whereas ν_6 is the only out-of-plane mode. Thus, if the coupling of ν_6 to the in-plane modes is controlled by weak or poorly resonant low-order anharmonic resonances, the energy in ν_6 is not available for penetration of the in-plane dissociation barrier. Consequently, each approximately isoenergetic trade of two quanta of ν_6 (900 cm^{-1}) for one quantum of ν_2 (1700 cm^{-1}) makes an additional 1800 cm^{-1} available to the in-plane modes as well as increases the anharmonic coupling matrix elements. This extreme mode sensitivity is also manifested in the much more rapid dissociation for $J \neq 0$ than $J = 0$ levels, due to activation of Coriolis-induced IVR mixing. Furthermore, this mechanism also explains the much slower dissociation rates for $J = 0$ levels of A″ (v_6 = odd) vs A″ (v_6 = even) vibrational symmetry: the v_6 = odd eigenfunctions have a node at the planar geometry that leads to zero probability along the minimum-energy (in-plane) dissociation path.

These SEP studies in HFCO provide perhaps the best example to date of nonstatistical, mode-specific dynamics in a polyatomic molecule at such high vibrational energy ($E_{VIB} < 22\,000$ cm^{-1}) and state densities (ρ > 10 states/cm^{-1}). These studies also provide at least one clear example of a more than 100-fold

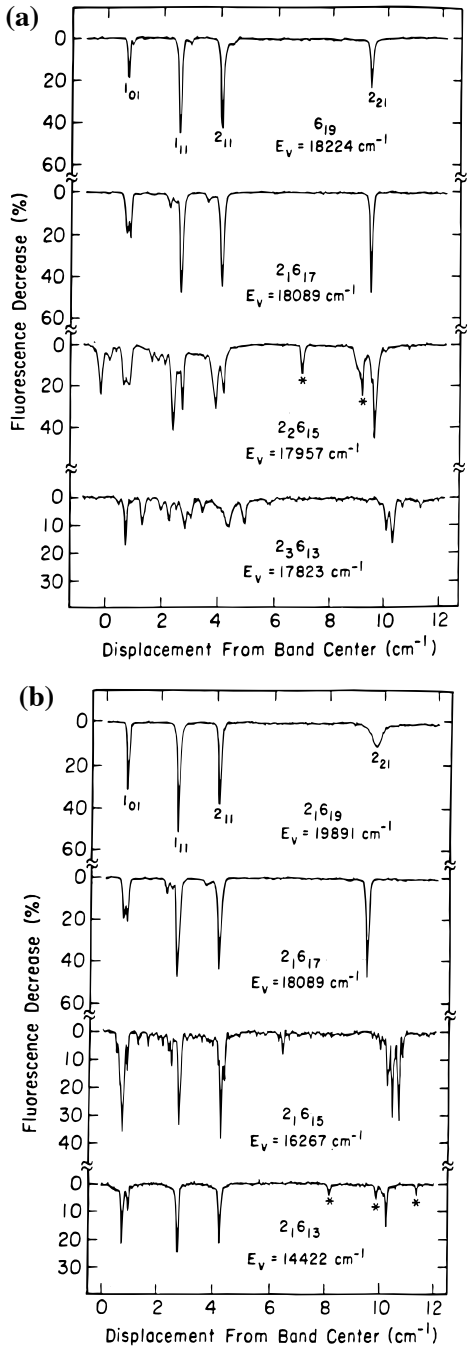

Figure 9. SEP spectra of HFCO demonstrating (a) the dramatic increase in IVR spectral fragmentation at roughly constant total excitation energy for increasing (decreasing) excitation of ν_2 (ν_6), respectively, and (b) the enhanced stability of extreme motion states for increasing excitation of ν_6. Reprinted with permission from ref 80. Copyright 1991 American Institute of Physics.

additional stability due to extreme versus distributed vibrational motion. Though not yet analyzed at the same level of detail, the decoupling of the out-of-plane ν_6 motion from the strongly coupled in-plane modes in HFCO is almost certainly a consequence of the weakness of low-order anharmonic resonances involving the ν_6 mode combined with the rapid growth in anharmonic couplings with successive ν_6 vibrational quanta, similar to effects observed previously at lower levels of vibrational excitation in both benzene and acetylene. Thus, the further analysis of HFCO should provide particularly helpful insights into the design of molecules where IVR and photodissociation rates can be "controlled" by excitation of a specific class of initial zero-order bright states.

B. IVR in Dissociating Species via Vibrationally Mediated Photodissociation. Although SEP has proven quite powerful in providing double-resonance Franck−Condon access to states both above and below the dissociation onset limit, it does require the molecule to have a suitably well-characterized, bound, electronically excited state. However, double-resonance studies can be extended to molecules without such bound electronically *excited* states by two-step pumping in the *ground* state, as demonstrated in the infrared−optical photofragmentation schemes of Rizzo and co-workers.[33−36] This class of double-resonance methods is based on the studies of the Crim group,[32,159,160] whereby $\Delta v = 5$ OH-stretch overtone excitation into the predissociative continuum of H_2O_2 could be monitored by LIF detection of the OH radical fragments. Similar one-photon methods have been implemented by King and co-workers[161] for overtone study of jet-cooled HN_3, probing the formation of NH radical by LIF. However, by splitting the excitation into two separate IR steps, Rizzo and co-workers have successfully extended these methods to probe the overtone absorption and dissociation spectra of fully *J , K, and vibrational-state-selected levels*. As the classic example, H_2O_2 can be (i) excited with an OPO to a selected *J*, *K* level of $\upsilon_{OH} = 1$ (or in combination with $\upsilon_{OO}/\upsilon_{OOH}$,), followed by (ii) tunable, overtone ($\Delta\upsilon_{OH} = 4$) excitation into the OH + OH predissociative continuum, which is subsequently monitored via (iii) LIF detection of the OH. The resulting double-resonance spectra are consistent with a simple parallel band of a prolate top, indicating that *K* is a meaningful quantum number on the time scale for IVR of the overtone ZOBS. However, extensive IVR clump structure due to mixing in the upper state is also observed, the *J* dependence of which indicates a density of coupled bath states that increases with overall rotation. Such data can be nicely explained from a tier model perspective, where there is predominantly *anharmonic* state mixing of the ZOBS with the first tier, but with strong Coriolis coupling into all successive tiers. It is also worth noting that similar trends have been reported in high-resolution IR studies of CH-stretch-excited hydrocarbons,[51−68] where such a "anharmonic + Coriolis-coupled bath" picture has been substantiated by a more quantitative spectroscopic analysis of the density of coupled states and the *J*,*K* dependence of matrix elements.[55,66,162]

C. Competition between IVR and Predissociation in Clusters. The excitation dynamics in H_2O_2 and HN_3 are characteristic of systems with both weak (O−O or N−N) and strong (O−H or N−H) bonds and where the flow of overtone excitation from the strong bond provides sufficient energy to fragment the molecule. The mere fact that IVR-induced clump structure can be resolved indicates that the coupling between the ZOBS and the first tier of dark states is stronger than the coupling between either class of bound state and the dissociation continuum. From a time-domain perspective, coherent excitation of the ZOBS would lead to a flow of the initially localized excitation into a bath of high-energy vibrational modes of the molecule, which in turn predissociate on a longer time scale. To the extent that these background levels are statistically mixed (recall that this does not occur, for example, in the extreme overtone states of HFCO),[79−82] the time scale for breaking the weak bond might therefore not be expected to demonstrate any dependence on the initial ZOBS excited.

A qualitatively different scenario is often observed in high-resolution spectroscopy of weakly bonded clusters, where even fundamental excitation in the near-IR is greatly in excess of the binding energy. Due to a combination of supersonic jet cooling and high-resolution light sources, rotationally resolved near-IR spectra have now been recorded for numerous dimer

(and larger cluster) systems, in which a smooth, Lorentzian broadening of widely separated rovibrational transitions is routinely observed.[115−118] Though these line shapes could *in principle* be due to IVR coupling to a dense manifold of vibrationally metastable levels that eventually dissociate on a longer time scale, this would require state densities typically many orders of magnitude larger than reasonable. Indeed, in the few cases where direct time- and frequency-domain comparisons have been possible (e.g., NO dimer),[163,164] the time-domain appearance rates and frequency-domain line widths agree to within experimental certainties, indicating that predissociative rupturing of the weak bond occurs "directly". By way of contrast, if the spectroscopic widths were dominated by rapid IVR into long-lived dark states, then the time-domain appearance rates could be arbitrarily slower than suggested by the inverse of the frequency-domain line widths. It is not surprising, therefore, that many of these weakly bound dimer systems demonstrate predissociation rates that are strongly mode- and quantum-state specific. For example, in the well-studied hydrogen halide dimer systems where one can unambiguously distinguish H bond "donor" and "acceptor" localized stretching vibrations, the excitation of the "donor" stretch leads to a predissociation rate that is as much as 50-fold faster than the corresponding "acceptor" stretch.

However, this simple Fourier transform connection between frequency-domain line widths (particularly measured at insufficient resolution) and dissociation rates in clusters is not always valid, as was eventually shown to be the case in the ethylene dimer system. In these clusters, broad homogeneous line widths of order 50 cm^{-1} are observed in the CH bend region from *low-resolution*, line-tunable CO_2 laser studies[120−122] which had originally been interpreted as resulting from rapid predissociation on the subpicosecond time scale. However, later studies with tunable *high-resolution* laser sources[123,124] revealed that this 50 cm^{-1} broad line width splits into extensively fractionated "clump" spectral structures quite characteristic of extensive IVR. Furthermore, the intrinsic predissociation line widths in this IVR fine structure proved to be laser limited to <30 MHz, i.e., at least 50 000 times narrower than the band associated with the CH bend ZOBS oscillator strength. Thus, coherent excitation of the CH bend ZOBS in ethylene dimer leads to IVR relaxation at least 4−5 orders of magnitude faster than eventual predissociation into the translational continuum.

A particularly clean example of significant differences between IVR and dissociation rates is provided by near-IR spectra of the DF trimer,[119] for which several distinct regions of configuration space can be accessed via near-IR excitation. There is a predicted C_{3h} cyclic ring structure for the ground state,[165] which upon DF stretch excitation might in principle break *two* hydrogen bonds to form $(DF)_2$ + DF or *one* hydrogen bond to access a highly floppy, "linear" isomer region of phase space. The corresponding near-IR-stretch excitation of HF trimer accesses *both* two and three hydrogen-bond-breaking channels.[166] Even under high-resolution supersonic jet conditions, the HF trimer spectrum yields no discernible rotational structure[167,168] ostensibly due to rapid (subpicosecond) predissociation into the continuum. The high-resolution IR spectrum of the DF trimer proves to be qualitatively quite different, with clear rotational *K* progressions characteristic of a perpendicular band of a cyclic symmetric top structure (see Figure 10). Indeed, the vibrational averaged molecular structure inferred from a rotational analysis of the spectrum is in remarkably quantitative agreement with theoretical predictions. This isotopic dependence of the predissociation rate is certainly due to a lower DF-stretching frequency as well as the greater stability

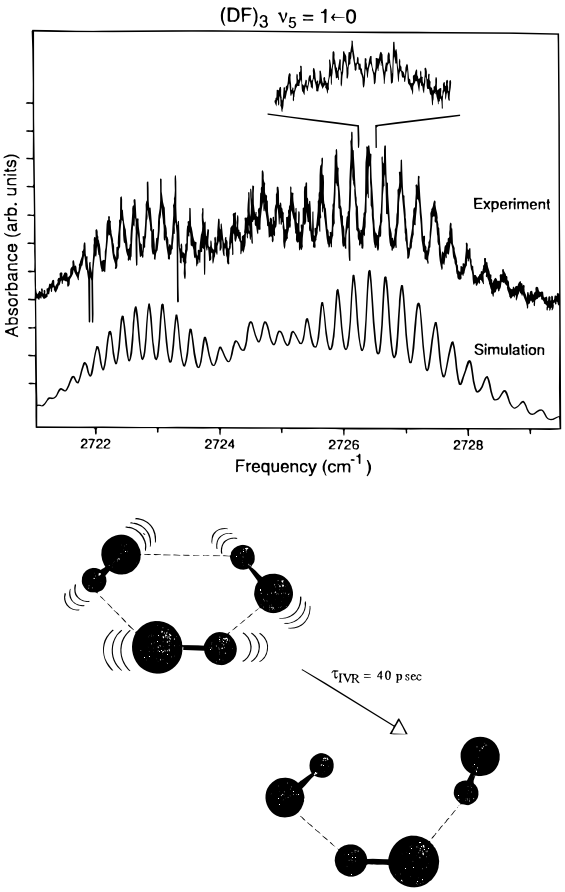

Figure 10. High-resolution jet-cooled spectra of the ν_5 asymmetric DF-stretch band of the $(DF)_3$ hydrogen-bonded cluster (ref 119). The overall band contour is characteristic of a D_{3h} cyclic structure, but multiple high-resolution scans illustrate a reproducible spectral fine structure several thousandfold more dense than anticipated for a "rigid" molecule at these 10 K temperatures. This structure corresponds to IVR mixing of the DF stretch with the ring modes. This mixing provides excitation energy sufficient to break one hydrogen bond in the ring to form the entropically much more favored "floppy" linear isomer on the 40 ps time scale.

of the zero-point level, which dramatically slows (and possibly even energetically closes)[166] the predissociation channel.

However, the *smooth* line shapes in the least-squares spectral simulation shown in Figure 10 require convolution of a 0.13 cm^{-1} homogeneous component with each predicted rotational line. Such an interpretation would be consistent, for example, with 40 ps predissociative broadening in the upper state. At even higher resolution (see inset in Figure 10), one finds dense *fine structure* (∼30 MHz) in the DF trimer spectrum, which is quite reproducible and several orders of magnitude more congested than predicted from any "rigid" molecular model. This excess sharp structure has been modeled by random matrix analysis[119] to infer the distribution of coupled states and coupling matrix elements; this analysis indicates a density of bath states of 20−30-fold larger than can be predicted from the vibrational-state density alone, but is well reproduced by a spectral model that assumes a strongly Coriolis-coupled bath with loss of K_a and K_c as good quantum numbers. Thus, the spectra clearly illustrate a case where the IVR coupling between the DF stretch (i.e., the ZOBS) and the bath modes is considerably stronger than any subsequent coupling to the predissociation continuum. Furthermore, we know something about the statistical nature of the excited bath modes; at $E_{VIB} \approx 2900$ cm^{-1}, the state density is dominated by low-frequency vibrations of a more "open" DF−DF−DF structure of the DF trimer, whereby configurations with only two hydrogen bonds are significantly accessed.

Conversely, the fraction of rovibrational states corresponding to excitation low enough to maintain all three hydrogen bonds intact is sufficient to account for only $\lesssim 5\%$ of the observed line density in the spectrum. A simple physical picture of vibrational energy flow dynamics in the time domain is therefore that the IVR clump structure reflects the breaking of *one* hydrogen bond and the consequent *opening of the ring*, which from the observed IVR widths (0.13 cm^{-1}) takes place on a 40 ps time scale. Interestingly, this ring opening for DF *trimer* occurs 10−100 times *faster* than the time scale for predissociation in DF *dimer*,[169] which also occurs via single hydrogen-bond cleavage. This large difference in rates may therefore reflect the influence of ring *strain* in the hydrogen-bond-breaking dynamics.

D. IVR and Possible Spectral Signatures of Isomerization. The above high-resolution studies of large-amplitude motion and IVR relaxation in clusters raise an interesting question. What are the frequency- and time-domain "signatures" associated with surmounting a barrier to unimolecular rearrangement (i.e., isomerization) for "stable" molecules? Starting at the most naive level, one might expect a discontinuous increase in the density of vibrational states and a corresponding decrease in the average intensity per resolved spectral line. A potential energy maximum or saddle point would wreak havoc on the frequencies and internal displacement coordinate composition of at least two vibrational modes, possibly causing gross changes in the resonance structure on which the scaling of the vibrational polyad patterns is based and thus causing spectral "unzipping" procedures to break down. The hierarchical tier structure, as measured by statistical procedures pioneered by Davis,[83] would change, possibly abruptly. Perhaps at the most subtle but universal level, identical atom permutation splittings would begin to appear in the high-resolution spectrum. Returning to the case of acetylene, each zero-order vinylidene vibrational level acts as a transition state "resonance" for permutation of identical H and C atoms in acetylene, e.g., $H_a-C_b\equiv C_c-H_d \leftrightarrow H_d-C_b\equiv C_c-H_a$. In the case of $^{12}C_2H_2$ and $^{12}C_2D_2$, the $I = 0$ nuclear spins of ^{12}C lead to zero statistical weight for one member of every permutation doublet; thus, only tunneling *shifts* rather than explicit tunneling *splittings* would be observable. However, for $^{13}C_2H_2$ and $^{13}C_2D_2$, both members of each permutation−inversion−tunneling doublet would be resolvable in high-resolution spectra of the dark states with appreciable vinylidene character; the pattern of doublet splittings (and the statistical weights of the doublet components) should therefore provide a mechanism for locating zero-order vibrational levels of the unstable vinylidene isomer. Such permutation splittings have been observed by Oka et al.[170] in the infrared spectrum of $C_2H_3^+$, where large-amplitude motion of the three protons mimics similar isomerization pathways and dynamics at much lower E_{VIB}.

VI. Predicting and Controlling IVR

A. Toward a Moiety-Specific Description of IVR. The rapid evolution of new experimental and theoretical techniques in the study of IVR has facilitated enormous progress in the past 10 years. However, we are still in a relatively early stage with regard to developing *predictive* capability in as yet unstudied systems. Specifically, we know a great deal about a handful of prototypic systems over an experimentally accessible window of energies. One of many important challenges remaining is to develop robust, detailed models of IVR that shift the focus from explanation toward prediction, not only of the *initial rates* of energy flow but also of the various *pathways* by which the energy flow flows.

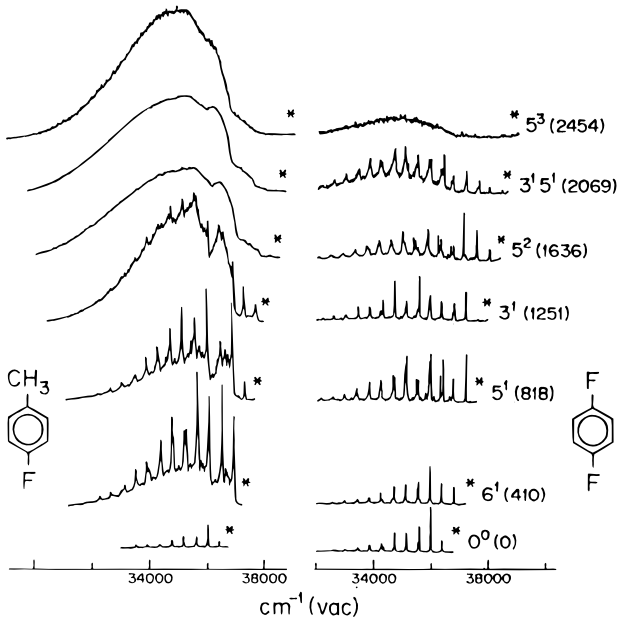

Figure 11. The presence of a methyl group profoundly influences IVR in *p*-fluorotoluene (*p*FT) vs *p*-difluorobenzene (*p*DFB), as illustrated in studies by Parmenter and Stone[171] as a function of energy above the S_1 origin. The much lower energy onset of the broad versus sharp dispersed fluorescence in *p*FT versus *p*DFB is ascribed to methyl rotor "acceleration" of the IVR rates by as much as 100-fold. Reprinted with permission from ref 171. Copyright 1986 American Institute of Physics.

One very attractive possibility suggested by many of the studies cited in this review is that the early time IVR can be described adequately by a more "local" treatment of the dynamics. For example, the initial fast relaxation in CH-stretch-excited benzene[86−88] was explained by local stretch−bend Fermi resonance interactions localized on a single CH group, as was also observed in overtone CH-stretch levels of substituted methanes.[41−45] Similarly, the time scale for the decay of CH-stretch excitation in terminal acetylenes appears to be characteristic of the CCH moiety and remarkably insensitive to the rest of the molecular structure or vibrational state density.[52,57−59] As both chemists and spectroscopists, we routinely rely on intuitive notions based on similar "functional group" analyses; if IVR rates prove to be predictively characterized by such a functional group or moiety-specific analysis, this would represent a conceptual advance of enormous magnitude. Though we have not yet arrived at such a picture, we have already begun to recognize some of the important mileposts along the way.

B. Methyl Rotor Acceleration of IVR. There has been significant evidence accumulated for the "accelerating" effect of a single methyl rotor substituent on IVR processes in electronically excited aromatic ring species. This has been studied most extensively by comparisons between *p*-fluorotoluene (*p*FT) and *p*-difluorobenzene (*p*DFB) by Parmenter and co-workers,[171−175] using single vibronic level excitation followed by dispersed fluorescence. In a fashion analogous to the original analysis of alkylbenzenes by Smalley and co-workers,[16−18] the relative contribution from resonance fluorescence (sharp) and relaxed fluorescence (broad) is taken as a measure of the IVR rate in the upper state. The results (see Figure 11) indicate a remarkable, nearly 2 orders of magnitude increase in IVR rates upon methyl group substitution. The magnitude of this increase can be semiquantitatively explained by a model of unimolecular "collisions" between the vibrating ring and methyl rotor,[172,175] which permit the enormous number of additional states associated with the rotor motion to contribute, from a Fermi Golden Rule perspective, to the effective density of IVR-coupled

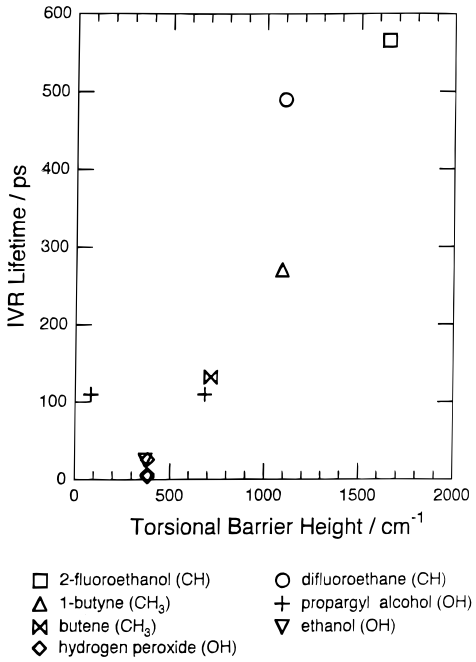

Figure 12. Dependence of IVR lifetimes on torsional barrier height for isomerization, indicating the important role of large-amplitude skeletal motions in promoting IVR. Reprinted with permission from ref 68. Copyright 1995 VCH.

states.[176] Further theoretical analyses by Martens and Reinhardt[177] emphasize that the coupling between methyl rotation and low-frequency ring modes is crucial to the promotion of this vibrational state mixing.[178,179] It is appropriate to mention, however, that no such methyl rotor acceleration effects have been explicitly evident in the high resolution IR studies of CH-stretch-excited terminal acetylenes.[51−63]

C. Skeletal Torsion as an IVR Accelerator. The influence of large-amplitude methyl rotor motion on IVR suggests that similar effects might also arise from other large-amplitude torsional modes, such as around single C−O and C−C bonds. The effects of such generalized centers of flexibility (COF) on IVR state mixing have been studied in high-resolution IR laser absorption studies of CH- and OH-stretch-excited hydrocarbons by several groups.[52,54,65,69] The analysis of Perry et al.[65] suggests a clear correlation between *proximity* of the stretch excitation to the center of flexibility and the fast initial IVR of the ZOBS (see Figure 12). For example, the $v_{CH} = 1$ methyl CH stretches in ethanol, which are two bonds away from the C−O center of flexibility, relax more slowly (59 ps) than the OH stretch directly attached to the COF (26 ps). Even larger ratios apply to the OH and acetylenic stretches in propargyl alcohol (CH_2OH−CCH) (110 and 500 ps, respectively), which are separated by one and three bonds from the only COF in the molecule (the C−C bond), respectively. A similar trend was also observed by McIlroy and Nesbitt in high-resolution studies of $v_{CH} = 1$ excitation of 1-pentyne,[52,53] in which a more than 1 order of magnitude increase in IVR rates is exhibited for methyl versus acetylenic CH-stretch excitations. Of course, one could argue that this difference is a consequence of the difference between aliphatic and acetylenic CH-stretch moieties. However, if the 1-pentyne carbon chain is reduced by one methylene group to 1-butyne, the C−C−C skeletal torsional coordinate (COF) disappears, and the methyl CH-stretch IVR lifetime increases by nearly 10-fold.

A particularly relevant example of this effect has been noted in isomer comparison studies[54] of 1-butene and *trans*-2-butene. Both of these species have 30 vibrational degrees of freedom

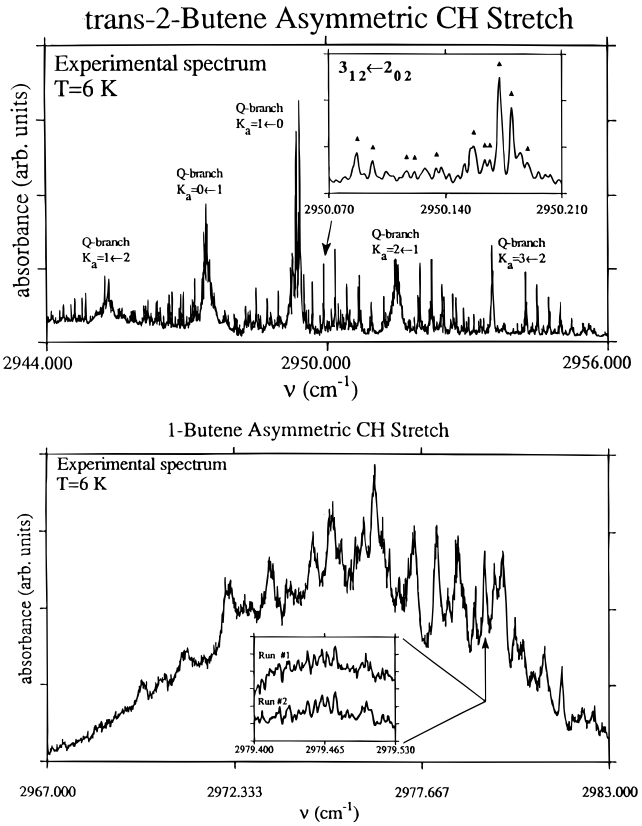

Figure 13. High-resolution jet-cooled (10 K) spectra (ref 54) in the asymmetric stretch region of *trans*-2-butene and 1-butene, demonstrating the importance of low-energy barriers to skeletal isomerization in promoting IVR. Both hydrocarbons have 30 degrees of freedom and a total state density of approximately 200 states/cm^{-1} at CH-stretch excitation energies. Nevertheless, the "rigid" *trans*-2-butene skeleton leads to a fully resolved spectrum at high resolution, whereas the "floppy" 1-butene spectrum is unresolved, with evidence of at least a 20−30-fold greater density of mixed states than for *trans*-2-butene.

and comparable densities of states (215 and 170 states/cm^{-1}) at $v_{CH} = 1$ methyl CH-stretch-excitation energies. The essential structural difference between these two molecules is that the carbon chain in 1-butene is "floppy" with a low barrier to C−C−C torsional isomerization, whereas the *trans*-2-butene framework is essentially "rigid" due to the central double bond. From a vibrational perspective, the differences involve a substitution of one *skeletal* torsion in 1-butene for one *methyl* torsion in *trans*-2-butene, which therefore provides a basis for isolating and comparing the effects of these two large-amplitude modes on the IVR rates. As shown in Figure 13, this substitution results in a dramatic change in the high-resolution jet-cooled spectra. Specifically, the *trans*-2-butene spectrum shows resolved and assignable rotational structure, whereas the 1-butene spectrum exhibits a "continuous" profile structure even at sub-Doppler (0.001 cm^{-1}) resolution and 6 K rotational temperatures. However, as was observed in the DF trimer spectrum,[119] the apparent "noise" in the 1-butene spectrum is quite real, as demonstrated by repeated scans (see inset) over the same spectral region. Analysis of the spectral fine structure reveals overlapping bath levels at a density 20−30-fold larger than observed in *trans*-2-butene and directly reflects the influence of a (light) methyl rotor vs a (heavy) C−C−C skeletal torsion on IVR dynamics. It is also worth noting that this 20−30-fold increase in coupled state density is similar to what was measured in DF trimer spectrum,[119] which could be attributed to essentially complete Coriolis mixing of K levels in the dark state manifold.

This suggests the following simple picture for CH-stretch IVR dynamics in systems with centers of flexibility. First, we can safely assume that IVR anharmonic state mixing of the CH-stretch ZOBS occurs with essentially all vibrationally isoenergetic states in *both* butenes (this has proven to be the case in all CH-stretch-excited systems analyzed at high resolution thus far).[3,52−66] However, the nature of the corresponding bath states is quite different for the two species; from a direct state count, almost half of the bath states in *1-butene* already lie *above* the C−C−C torsional barrier that controls the interconversion of the two skew isomers. Due to the large dependence of rotational constants on the torsional coordinate, these zero-order bath states in *1-butene* will be highly mixed by Coriolis and rotation−vibration coupling. This qualitatively explains the 20−30-fold increase in density of coupled states observed between the two species, though relatively comparable clump widths and IVR lifetimes are inferred from the two spectra. In essence, the presence of a low-barrier C−C−C torsional coordinate in the "floppy" 1-butene opens an additional channel for rotationally induced IVR state mixing not present in the "rigid" *trans*-2-butene isomer. Physically, the strong dependence of moments of inertia on the internal C−C−C torsional degree of freedom provides an efficient mechanism for coupling between rotational and low-frequency vibrational motion.[180,181]

D. IVR Modification by Blocking Groups. The bulk of spectral evidence from high-resolution studies indicates that IVR rates are dominated by the first tier in a hierarchical sequence of relaxation paths but are in general very poorly correlated with the total density of states. These first-tier "doorway" states have the physical interpretation as arising from the zero-order vibrations that are most strongly coupled via low-order anharmonic resonances to the initially localized ZOBS excitation. Since from a perturbative framework the strength of this resonance coupling would be expected to be related to geometric proximity, this immediately suggests the possibility of influencing IVR rates by virtue of "local" modifications of molecular structure. One specific example of this has been whether CH-stretch IVR can be slowed by the presence of "blocking" groups in a linear chain, as theoretically studied by Hutchinson et al.[89,90] By virtue of both the "peninsular" nature of the CH group and the highly localized nature of the ZOBS, CH-stretch-excited terminal acetylenes have once again proven to be ideal systems for such theories of IVR energy flow down a chain. This has been tested in beautiful studies by Lehmann, Scoles, and co-workers,[3,57,58] who investigated CH-stretch IVR rates in a series of terminal acetylenes of the general form $(CY_3)_3X-CCH$. By adjusting X from C to Si to Sn, they could systematically vary the mass of the central atom in an attempt to block the terminal acetylene from the predominant source of state density in the substituted trimethyl end of the molecule. The results, summarized in Table 2, indicate over an order of magnitude *decrease* of IVR rate upon Si or Sn substitution for C. Less sensitivity to the Y substituent is noted, but the general trend toward slightly increased rates with greater density of background levels is clear.

One might be concerned that any change in the molecular structure represents too much of a change to be considered "perturbative". However, with access to both 2.7 and 1.5 mm laser sources, Lehmann, Scoles, and co-workers could also obtain IVR rates for both $v_{CH} = 1$ and $v_{CH} = 2$, thereby isolating the effect of state density on IVR dynamics for the same molecular structure. The results in Table 2 indicate only quite modest changes (typically 2-fold decreases) in IVR rates, despite the 10^3-10^5 increase in vibrational state density. Indeed, there are even indications in some of these systems that overtone excitation *slows* IVR rates, which would be consistent with the notion of additional stability in extreme motion states. Interestingly, there are indications[56] from other high-resolution CH-stretch studies of precisely the opposite trend, e.g., IVR rates are *slower* for $v_{CH} = 2$, $v'_{CH} = 1$ excitation of diacetylene than for $v_{CH} = 3$, $v'_{CH} = 0$. However, diacetylene most likely represents a special case because of the extreme decoupling effects of terminal acetylenes. Essentially, the two CH groups in diacetylene are so well isolated from each other that one expects the combination level to sample less anharmonic regions of the potential surface and thus be more stable with respect to IVR mixing than the isoenergetic pure overtone.

E. Toward an *ab Initio* Based Theoretical Description of IVR. The combined set of high-resolution studies of terminal acetylenes provides a richly varied set of test systems for comparison with detailed theoretical predictions. Of special note in this regard is the work by Stuchebrukov and Marcus,[85] which has successfully reproduced all of the observed trends with semi-quantitative reliability. Their approach is computationally tractable, utilizes physically reasonable assumptions, and is based on empirical and *ab initio* input. This is in many ways related to the work by Wyatt and co-workers[93−97] on IVR relaxation in CH-stretch-excited benzene, but succeeding on qualitatively longer time scales (1 ns versus 100 fs) for the resulting dynamics in terminal acetylenes.

Specifically, Stuchebrukov and Marcus have studied CH fundamental and overtone relaxation in the $(CY_3)_3X-CCH$ family of molecules, based on a tier model with cubic and quartic anharmonic couplings transferred from empirical and/or *ab initio* studies of smaller molecules with the same functional group.[85] The zero-order basis set is taken from normal-mode analysis, where the criterion for membership in a specific tier is based on low-order, near-resonant anharmonic coupling. The zero-order tier (T_0) contains the ZOBS (either $v_{CH} = 1$ or 2). States in the nth tier are coupled to T_{n-1} and T_{n+1} by cubic anharmonicities and to the T_{n-2} and T_{n+2} tiers by quartic anharmonicities respectively, and limited to a resonance window (or order 100 cm^{-1}) between the coupled states. Projection operators are used to systematically eliminate redundant sampling of the same state in different tiers. Overall rotation and the extreme anharmonic effects of methyl rotor motions are neglected, but all 42 vibrational degrees of freedom are explicitly included. The model provides a reasonably simple algorithm for tier selection and analytic calculation of coupling matrix elements which is readily coded and consistent with an intuitive picture of IVR energy flow.[182,183] Furthermore, since the vibrational basis states in each tier and all coupling matrix elements are known, one can investigate IVR properties as function of total number of tiers, N. Thus, one can prediagonalize the first N tiers (within an energy window to limit the matrix size) and thereby predict average state densities and root mean square matrix elements and test for convergence in the IVR line widths and lifetimes via Fermi's Golden Rule.

The predicted IVR lifetimes (see Table 2) prove to be in rather good agreement with experimental results and yet adequately converged with respect to the number of tiers included in the calculation. Specifically, the order of magnitude *decrease* in IVR rates with Si versus C and the more modest increases between $v_{CH} = 2$ and $v_{CH} = 1$ excitation and H/D substitution are well reproduced. The overall magnitudes of the IVR widths (0.01 cm^{-1}) are in a qualitatively different regime than for relaxation of $v_{CH} = 3$ overtones in benzene (5 cm^{-1}) and more consistent with a dynamical tunneling picture first introduced by Heller and Davis.[99,100] The remarkable success of such a hybrid empirical/*ab initio* calculation in reproducing experi-

mental results bodes well for a *mechanistic* understanding of IVR, more or less based on first principles, as well as further development of quantitative IVR models in the near future. For example, since the calculations can be simply repeated on the same anharmonic potential surface for an effective mass 28 (i.e., mimicking Si), the purely kinematic influence of "blocking" groups can be theoretically isolated. The Stuchebrukov and Marcus calculations[85] clearly show that, although an effective mass 28 C atom would decrease the average coupling-matrix elements, the much greater increase in the number of low-order anharmonic resonances more than compensates for this change and thereby significantly increases IVR rates. Thus, an increase in mass by itself would lead to an "inverse blocking" effect. The observed decrease in IVR rates in the Si versus C systems is instead explained by an anomalously small density of low-order, anharmonically coupled states for low-tier numbers, which produces an effective "bottleneck" in the vibrational energy flow. It is worth noting that this is contrary to predictions based on *total* state density, which increases 30-fold from C to Si. This underscores the physical insight that can be extracted from a tier-based description of IVR dynamics, as well as the relative unimportance of total vibrational state density as a control parameter for IVR time scales.

VII. Summary and Concluding Remarks

Although a detailed understanding of IVR has been one of the long-standing, major goals in physical chemistry over the past decades, this has proven to be a far larger challenge than originally appreciated, and there is still very much yet to be learned. However, as this review has tried to capture, there have also been some particularly striking advances in recent years, both theoretically and experimentally, that are starting to offer real hope for a *predictive* understanding of this ubiquitous and important phenomenon. Fueling this optimism are the efforts in which experiment and theory have both evolved in sophistication *toward one another* so as to facilitate the most direct and rigorous comparison possible. Experimentally, this has taken the form of eliminating or decreasing the extent of averaging over quantum state distributions by multiple-resonance state labeling, high-resolution light sources, and/or jet cooling or conversely by systematically isolating and extracting the early dynamics from a complicated energy transfer pathway in the time domain. Theoretically, this has been facilitated by both demonstration of "local" moiety-specific paradigms for IVR energy flow and rapid computational developments that are beginning to permit IVR rates and pathways in relatively complicated and realistic systems to be calculated from first principles. From these many recent successes, it seems likely that the focus of efforts will soon be able to shift from that of explanation (i.e., can we understand how IVR occurs) to one of manipulation (i.e., can we control IVR, by molecular design or method of excitation) of the basic energy-flow pathways. In any event, one can safely speculate that the next decade offers many opportunities for exciting new applications in the field of IVR.

Acknowledgment. This work has been supported by funds from the National Science Foundation, the Air Force Office of Scientific Research, and the Department of Energy.

References and Notes

(1) Parmenter, C. S. *Faraday Discuss. Chem. Soc.* **1983**, *75,* 7.
(2) McDonald, J. D. *Annu. Rev. Phys. Chem.* **1979**, *30,* 29.
(3) Lehmann, K. K.; Scoles, G.; Pate, B. H. *Annu. Rev. Phys. Chem.* **1994**, *45,* 241.
(4) (a) Quack, M. *Annu. Rev. Phys. Chem.* **1990**, *41,* 839. (b) Quack, M.; Kutzelnigg, W. *Ber. Bunsen-Ges. Phys. Chem.* **1995**, *99,* 231.
(5) Knight, A. E. W. *Ber. Bunsen-Ges. Phys. Chem.* **1988**, *92,* 337.
(6) Felker, P. M.; Zewail, A. H. In *Jet Spectroscopy and Molecular Dynamics;* Hollas, J. M.; Phillips, D., Eds.; Blackie A&P: London, 1995.
(7) Child, M. S.; Halonen, L. *Adv. Chem. Phys.* **1984**, *57,* 1.
(8) Uzer, T. *Phys. Rep.* **1991**, *199,* 124.
(9) Robinson, G. W. *J. Chem. Phys.* **1967**, *47,* 1967.
(10) Marcus, R. A. *J. Chem. Phys.* **1952**, *20,* 258.
(11) Robinson, P. J.; Holbrook, K. A. In *Unimolecular Reactions*; Wiley: New York, 1972.
(12) Metz, R. B.; Thoemke, J. D.; Pfeiffer, J. M.; Crim, F. F. *J. Chem. Phys.* **1993**, *99,* 1744.
(13) Sinha, A.; Thoemke, J. D.; Crim, F. F. *J. Chem. Phys.* **1992**, *96,* 372.
(14) Simpson, W. R.; Girard, B.; Zare, R. N. *J. Chem. Phys.* **1991**, *95,* 8647.
(15) Bar, I.; Cohen, Y.; David, D.; Rosenwaks, S.; Valentini, J. J. *J. Chem. Phys.* **1990**, *93,* 2146.
(16) Hopkins, J. B.; Powers, D. E.; Smalley, R. E. *J. Chem. Phys.* **1980**, *72,* 5039.
(17) Hopkins, J. B.; Powers, D. E.; Mukamel, S.; Smalley, R. E. *J. Chem. Phys.* **1980**, *72,* 5049.
(18) Hopkins, J. B.; Powers, D. E.; Smalley, R. E. *J. Chem. Phys.* **1980**, *73,* 683.
(19) Kommandeur, J.; Majewski, W. A.; Meerts, W. L.; Pratt, D. W. *Annu. Rev. Phys. Chem.* **1987**, *38,* 433.
(20) Siebrand, W.; Meerts, W. L.; Pratt, D. W. *J. Chem.* **1989**, *90,* 1313.
(21) Lawrance, W. D.; Knight, A. E. W. *J. Phys. Chem.* **1985**, *89*, 917.
(22) Felker, P. M.; Zewail, A. H. *J. Chem. Phys.* **1985**, *82,* 2961.
(23) Felker, P. M.; Zewail, A. H. *J. Chem. Phys.* **1985**, *82,* 2975.
(24) Felker, P. M.; Zewail, A. H. *J. Chem. Phys.* **1985**, *82*, 2994.
(25) Felker, P. M.; Zewail, A. H. *J. Chem. Phys.* **1985**, *82,* 3003.
(26) Lambert, W. R.; Felker, P. M.; Zewail, A. H. *J. Chem. Phys.* **1981**, *75,* 5958.
(27) Matsumoto, Y.; Spangler, L. H.; Pratt, D. W. *Laser Chem.* **1983**, *2,* 91.
(28) Van der Meer, J.; Jonkman, H. Th.; Kommandeur, J.; Meerts, W. L.; Majewski, W. A. *Chem. Phys. Lett.* **1982**, *92,* 565.
(29) (a) Bixon, M.; Jortner, J. *J. Chem. Phys.* **1968** *48,* 715. (b) Amirav, A.; Even, U.; Jortner, J. *J. Phys. Chem.* **1982**, *86,* 3345.
(30) Stannard, P. R.; Gelbhart, W. M. *J. Phys. Chem.* **1981**, *85,* 3592.
(31) Moore, C. B.; Weisshaar, J. C. *Annu. Rev. Phys. Chem.* **1983**, *34,* 525.
(32) Rizzo, T. R.; Hayden, C. C.; Crim, F. F. *Faraday Discuss. Chem. Soc.* **1975**, *75,* 223.
(33) Luo, X.; Rizzo, T. R. *J. Chem. Phys.* **1992**, *96,* 5659.
(34) Boyarkin, O. V.; Settle, R. D. F.; Rizzo, T. R. *Ber. Bunsen-Ges. Phys. Chem.* **1995**, *99,* 504.
(35) Fleming, P. R.; Li, M.; Rizzo, T. R. *J. Chem. Phys.* **1991**, *94,* 2425.
(36) Luo, X.; Fleming, P. R.; Seckel, T. A.; Rizzo, T. R. *J. Chem. Phys.* **1990**, *93,* 9194.
(37) Wong, J. S.; Moore, C. B. *J. Chem. Phys.* **1982**, *77,* 603.
(38) Jasinski, J. M.; Frisoli, J. K.; Moore, C. B. *Faraday. Discuss. Chem. Soc.* **1983**, *75,* 289.
(39) Wong, J. S.; Green, Jr., W. H.; Cheng, C.-K.; Moore, C. B. *J. Chem. Phys.* **1987**, *86,* 5994.
(40) Green, Jr., W. H.; Lawrance, W. D.; Moore, C. B. *J. Chem. Phys.* **1987**, *86,* 6000.
(41) Duebal, H.-R.; Quack, M. *Chem. Phys. Lett.* **1980**, *72,* 342.
(42) Amrein, A.; Duebal, H.-R.; Quack, M. *Mol. Phys.* **1985**, *56,* 727.
(43) Hollenstein, H.; Lewerenz, M.; Quack, M. *Chem. Phys. Lett.* **1985**, *165,* 175.
(44) (a) Duebal, H.-R.; Quack, M. *J. Chem. Phys.* **1984**, *81,* 3779. (b) Segall, J.; Zare, R. N.; Duebal, H.-R.; Lewerenz, M.; Quack, M. *J. Chem. Phys.* **1987**, *86,* 634.
(45) Lewerenz, M.; Quack, M. *J. Chem. Phys.* **1988**, *88*, 5408.
(46) Held, A.; Herman, M. *Chem. Phys.* **1995**, *190*, 407.
(47) Temsamani, M. A.; Herman, M. *J. Chem. Phys.* **1995**, *102*, 6371.
(48) There are many excellent examples in the special issue "Overtone Spectroscopy and Dynamics"; Lehmann, K. K., Herman, M., Eds.; *Chem. Phys.* **1995**, *190*.
(49) (a) Bray, R. G.; Berry, M. J. *J. Chem. Phys.* **1979**, *71*, 4909. (b) Reddy, K. V.; Berry, M. J. *Chem. Phys. Lett.* **1977**, *52*, 111.
(50) Hall, R. R. Ph.D. Thesis, Rice University, 1984.
(51) McIlroy, A.; Nesbitt, D. J. *J. Chem. Phys.* **1989**, *91*, 104.
(52) McIlroy, A.; Nesbitt, D. J. *J. Chem. Phys.* **1990**, *92*, 2229.
(53) McIlroy, A.; Nesbitt, D. J. In *Advances in Molecular Vibrations and Collision Dynamics 1A*; Bowman, J. M., Ed.; JAI Press: Greenwich, 1991; p 109.
(54) McIlroy, A.; Nesbitt, D. J. *J. Chem. Phys.* **1994**, *101*, 3421.
(55) McIlroy, A.; Nesbitt, D. J.; Kerstel, E. R. Th.; Pate, B. H.; Lehmann, K. K.; Scoles, G. *J. Chem. Phys.* **1994**, *100*, 2596.
(56) Gambogi, J. E.; Pearson, R. Z.; Yang, X.; Lehmann, K. K.; Scoles, G. *Chem. Phys.* **1995**, *190*, 191.

(57) Kerstel, E. R. Th.; Lehmann, K. K.; Mentel, T. F.; Pate, B. H.; Scoles, G. *J. Phys. Chem.* **1991**, *95*, 8282.
(58) Gambogi, J. E.; L'Esperance, R. P.; Lehmann, K. K.; Pate, B. H.; Scoles, G. *J. Chem. Phys.* **1993**, *98*, 1112.
(59) Gambogi, J. E.; Lehmann, K. K.; Pate, B. H.; Scoles, G.; Yang, X. *J. Chem. Phys.* **1993**, *98*, 1748.
(60) Pate, B. H.; Lehmann, K. K.; Scoles, G. *J. Chem. Phys.* **1991**, *95*, 3891.
(61) Gambogi, J.; Kerstel, E. R. Th.; Lehmann, K. K.; Scoles, G. *J. Chem. Phys.* **1994**, *100*, 2612.
(62) de Souza, A. M.; Kaur, D.; Perry, D. S. *J. Chem. Phys.* **1988**, *88*, 4569.
(63) Perry, D. S. *J. Chem. Phys.* **1993**, *98*, 6665.
(64) Bethardy, G. A.; Perry, D. S. *J. Chem. Phys.* **1993**, *98*, 6651.
(65) Bethardy, G. A.; Wang, X.; Perry, D. S. *Can. J. Chem.* **1994**, *72*, 652.
(66) Go, J.; Cronin, T. J.; Perry, D. S. *Chem. Phys.* **1993**, *175*, 127.
(67) Go, J.; Perry, D. S. *J. Chem. Phys.* **1992**, *97*, 6994.
(68) Perry, D. S.; Bethardy, G. A.; Wang, X. *Ber. Bunsen-Ges. Phys. Chem.* **1995**, *99*, 530.
(69) Fraser, G. T.; Pate, B. H.; Bethardy, G. A.; Perry, D. S. *Chem. Phys.* **1993**, *175*, 223.
(70) Fraser, G. T.; Pate, B. H. *J. Chem. Phys.* **1992**, *98*, 2477.
(71) Fraser, G. T.; Pate, B. H. *J. Chem. Phys.* **1994**, *100*, 6210.
(72) (a) Kittrell, C.; Abramson, E.; Kinsey, J. L.; McDonald, S.; Reisner, D. E.; Katayama, D.; Field, R. W. *J. Chem. Phys.* **1981**, *75*, 2056. (b) Hamilton, C. E.; Kinsey, J. L.; Field, R. W. *Annu. Rev. Phys. Chem.* **1986**, *37*, 493.
(73) Jonas, D. M.; Solina, S. A. B.; Rajaram, B.; Silbey, R. J.; Field, R. W.; Yamanouchi, K.; Tsuchiya, S. *J. Chem. Phys.* **1994**, *99*, 7350.
(74) Dai, H. L.; Korpa, C. L.; Kinsey, J. L.; Field, R. W. *J. Chem. Phys.* **1985**, *82*, 1688.
(75) Abramson, E.; Field, R. W.; Imre, D.; Innes, K. K.; Kinsey, J. L. *Chem. Phys.* **1984**, *80*, 2298.
(76) (a) Coy, S. L.; Chasman, D.; Field, R. W. In *Extracting Dynamical Information from Complex and Congested Spectra: Statistics, Pattern Recognition and Parsimonious Trees, Molecular Dynamics and Spectroscopy by Stimulated Emission Pumping*; Dai, H. L.; Field, R. W., Eds.; World Scientific: Singapore, 1994. (b) Field, R. W.; Coy, S. L.; Solina, S. A. B. *Prog. Theor. Phys.* **1994**, *116*, 143.
(77) Solina, S. A. B.; O'Brien, J. P.; Field, R. W.; Polik, W. F. *Ber. Bunsen-Ges. Phys. Chem.* **1995**, *99*, 555.
(78) Solina, S. A. B.; O'Brien, J. P.; Field, R. W.; Polik, W. F. *J. Phys. Chem.* **1996**, *100*, 7797.
(79) Choi, Y. S.; Moore, C. B. *J. Chem. Phys.* **1989**, *90*, 3875.
(80) Choi, Y. S.; Moore, C. B. *J. Chem. Phys.* **1991**, *94*, 5414.
(81) Choi, Y. S.; Teal, P.; Moore, C. B. *J. Opt. Soc. Am. B* **1990**, *7*, 1829.
(82) Moore, C. B.; Zheng, Q.-K.; Choi, Y. S.; Green, W. H.; Kim, S. K.; Mahoney, A. J.; Miller, W. H.; Pibel, C. D.; Polik, W. F.; Teal, P. *Philos. Trans. R. Soc. London, A* **1990**, *332*, 297.
(83) Davis, M. J. *J. Chem. Phys.* **1993**, *98*, 2614.
(84) Davis, M. J.; Bethardy, G. A.; Lehmann, K. K. *J. Chem. Phys.* **1994**, *101*, 2642.
(85) Stuchebrukhov, A. A.; Marcus, R. A. *J. Chem. Phys.* **1993**, *98*, 6044.
(86) Sibert, E. L., III; Reinhardt, W. P.; Hynes, J. T. *Chem. Phys. Lett.* **1982**, *92*, 455.
(87) Sibert, E. L., III; Reinhardt, W. P.; Hynes, J. T. *J. Chem. Phys.* **1984**, *81*, 1115.
(88) Sibert, E. L., III; Reinhardt, W. P.; Hynes, J. T. *J. Chem. Phys.* **1984**, *81*, 135.
(89) Hutchinson, J. S.; Reinhardt, W. P.; Hynes, J. T. *J. Chem. Phys.* **1983**, *79*, 4247.
(90) Hutchinson, J. S.; Hynes, J. T.; Reinhardt, W. P. *Chem. Phys. Lett.* **1984**, *108*, 353.
(91) Uzer, T.; Natanson, G. A.; Hynes, J. T. *Chem. Phys. Lett.* **1985**, *122*, 12.
(92) Uzer, T.; Hynes, J. T.; Reinhardt, W. P. *Chem. Phys. Lett.* **1985**, *117*, 600.
(93) Wyatt, R. E.; Iung, C.; Leforestier, C. *J. Chem. Phys.* **1992**, *97*, 3459.
(94) Wyatt, R. E.; Iung, C.; Leforestier, C. *J. Chem. Phys.* **1992**, *97*, 3477.
(95) Wyatt, R. E.; Iung, C. *J. Chem. Phys.* **1993**, *98*, 5191.
(96) Iung, C.; Wyatt, R. E. *J. Chem. Phys.* **1993**, *99*, 2261.
(97) Iung, C.; Leforestier, C.; Wyatt, R. E. *J. Chem. Phys.* **1993**, *98*, 6722.
(98) Heller, E. J. *Acc. Chem. Res.* **1981**, *14*, 368.
(99) Heller, E. J.; Davis, M. J. *J. Phys. Chem.* **1981**, *85*, 307.
(100) Heller, E. J. *J. Phys. Chem.* **1995**, *99*, 2625.
(101) Tannor, D. J.; Rice, S. A. *J. Chem. Phys.* **1985**, *83*, 5013. Tannor, D. J.; Rice., S. A. *Adv. Chem. Phys.* **1988**, *70*, 441.
(102) Shapiro, M.; Brumer, P. *J. Chem. Phys.* **1993**, *98*, 201.
(103) Judson, R. S.; Lehmann, K. K.; Rabitz, H.; Warren, W. S. *J. Mol. Struct.* **1990**, *223*, 425.
(104) Scherer, N. F.; Ruggiero, A. J.; Du, M.; Fleming, G. R. *J. Chem. Phys.* **1990**, *93*, 856.
(105) Chen, C.; Yin, Y.-Y.; Elliott, D. S. *Phys. Rev. Lett.* **1990**, *64*, 507.
(106) Park, S. M.; Lu, S.-P.; Gordon, R. J. *J. Chem. Phys.* **1991**, *94*, 8622.
(107) Chelkowski, S.; Bandrauk, A.; Corkum, P. B. *Phys. Rev. Lett.* **1990**, 2355.
(108) Krause, J. L.; Whitnell, R. M.; Wilson, K. R.; Yan, Y.-J.; Mukamel, S. *J. Chem. Phys.* **1993,** *99*, 6562.
(109) (a) Shaffer, W. H.; Nielson, A. H. *J. Chem. Phys.* **1941**, *9*, 847. (b) Strey, G.; Mills, I. M. *J. Mol. Spectrosc.* **1976**, *59*, 103.
(110) (a) Chaiken, J.; Gurnick, M.; McDonald, J. D. *J. Chem. Phys.* **1981** *74*, 106. (b) Chaiken, J.; Gurnick, M.; McDonald, J. D. *J. Phys. Chem.* **1981**, *74*, 117.
(111) (a) Brucat, P. J.; Zare, R. N. *J. Phys. Chem.* **1983**, *78*, 100. (b) Brucat, P. J.; Zare, R. N. *J. Chem. Phys.* **1984**, *81*, 2562.
(112) Cohen-Tanoudji, C.; Diu, B.; Laloe, F. *Quantum Mechanics*; Wiley: New York, 1977.
(113) Amrein, A.; Dubal, H.-R.; Lewerenz, M.; Quack, M. *Chem. Phys. Lett.* **1984**, *112*, 387.
(114) Burberry, M. S.; Albrecht, A. C. *J. Chem. Phys.* **1979**, *71*, 4768.
(115) Lehmann, K. K.; Smith, A. M. *J. Chem. Phys.* **1990**, *93*, 6140.
(116) Nesbitt, D. J. *Chem. Rev.* **1988**, *88*, 843.
(117) Nesbitt, D. J. *Annu. Rev. Phys. Chem.* **1994**, *45*, 367.
(118) Miller, R. E. *Acc. Chem. Res.* **1989**, *22*, 295.
(119) Suhm, M. A.; Farrell, J. T., Jr.; Ashworth, S. H.; Nesbitt, D. J. *J. Chem. Phys.* **1993**, *98*, 5985.
(120) Casassa, M. P.; Bomse, D. S.; Janda, K. C. *J. Chem. Phys.* **1981**, *74*, 504.
(121) Hoffbauer, M. A.; Liu, K.; Giese, C. F.; Gentry, W. R. *J. Chem. Phys.* **1983**, *78*, 5567.
(122) Fischer, G.; Miller, R. E.; Watts, R. O. *J. Phys. Chem.* **1984**, *88*, 1120.
(123) Snels, M.; Fantoni, R.; Zen, M.; Stolte, S.; Reuss, J. *Chem. Phys. Lett.* **1986**, *124*, 1.
(124) Baldwin, K. G. H.; Watts, R. O. *Chem. Phys. Lett.* **1986**, *129*, 236.
(125) Huisken, F.; Meyer, H.; Lauenstein, C.; Sroka, R.; Buck, U. *J. Chem. Phys.* **1986**, *84*, 1042.
(126) Peet, A. C.; Clary, D. C.; Hutson, J. M. *Chem. Phys. Lett.* **1986**, *125*, 477.
(127) Duschensky, F. *Acta Phys. Chem.* **1937**, *7*, 551.
(128) (a) Child, M. S. *Acc. Chem. Res.* **1985**, *18*, 45. (b) Kellman, M. E. *J. Chem. Phys.* **1986**, *85*, 6243.
(129) Davis, M. *J. Chem Phys. Lett.* **1992**,*192*, 479.
(130) Yamanouchi, K.; Ikeda, N.; Tsuchiya, S.; Jonas, D. M.; Lundberg, J. K.; Adamson, G. W.; Field, R. W. *J. Chem. Phys.* **1991**, *95*, 6330.
(131) Jonas, D. M.; Solina, S. A. B.; Rajaram, B.; Silbey, R. J.; Field, R. W.; Yamanouchi, K.; Tsuchiya, S. *J. Chem. Phys.* **1992**, *97*, 2813.
(132) Gomez Florente, J. M.; Farantos, S. C.; Hahn, O.; Taylor, H. S. *J. Opt. Soc. Am.* **1990**, *B7*, 1851.
(133) Frederick, J. H.; Heller, E. J.; Ozment, J. L.; Pratt, D. W. *J. Chem. Phys.* **1988**, *88*, 2169.
(134) Kemper, M. J. H.; Van Dijk, J. M. F.; Buck, H. M. *Chem. Phys. Lett.* **1978**, *53*, 121.
(135) Whitten, G. Z.; Rabinovitch, B. S. *J. Chem. Phys.* **1963**, *38*, 2466.
(136) Forst, W. *Chem. Rev.* **1971**, *71*, 339.
(137) Porter, C. E. *Statistical Theories of Spectral Fluctations*; Academic: New York, 1965.
(138) Wigner, E. P. *Phys. Rev.* **1932**, *40*, 749.
(139) Berry, M. V.; Tabor, M. *Proc. Phys. Soc. London, Ser.* **1977**, *A356*, 375.
(140) Scherer, N. F.; Matro, A.; Ziegler, L. D.; Du, M.; Carlson, R. J.; Cina, J. A.; Fleming, G. R. *J. Chem. Phys.* **1992**, *96*, 4180.
(141) Scherer, N. F.; Carlson, R. J.; Matro, A.; Du, M.; Ruggiero, A. J.; Romero-Rochin, V.; Cina, J. A; Fleming, G. R.; Rice, S. A. *J. Chem. Phys.* **1991**, *75,* 1487.
(142) Stewart, G. M.; McDonald, J. D. *J. Chem. Phys.* **1983**, *78,* 3907.
(143) Kulp, T. J.; Ruoff, R. S.; McDonald, J. D. *J. Chem. Phys.* **1985**, *82*, 2175.
(144) Kulp, T. J.; Kim, H. L.; McDonald, J. D. *J. Chem. Phys.* **1986**, *85,* 211.
(145) Minton, T. K.; Kim, H. L.; Reid, S. A.; McDonald, J. D. *J. Chem. Phys.* **1988**, *89,* 6550.
(146) Nesbitt, D. J.; Leone, S. R. *Chem. Phys. Lett.* **1982**, *87,* 123.
(147) Pine, A. S.; Lafferty, W. J. *J. Res. Natl. Bur. Stand.* **1982**, *87*, 237.
(148) Tandy, D. C.; Larson, C. W.; Rabinovitch, B. S. *Can. J. Chem.* **1968**, *46,* 341.
(149) Larson, C. W.; Rabinovitch, B. S. *J. Chem. Phys.* **1961**, *51,* 2293.
(150) Hirschfelder, J. O.; Curtiss, C. F.; Bird, R. B. In *Molecular Theory of Gases and Liquids;* Wiley: New York, 1954.

(151) Lehmann, K. K.; Coy, S. L. *J. Chem. Soc., Faraday Trans.* **1988**, *84*, 1389.
(152) Coy, S. L.; Lehmann, K. K. *J. Chem. Phys.* **1986**, *84*, 5239.
(153) Holland, J. K.; Newnham, D. A.; Mills, I. M. *Mol. Phys.* **1990**, *70*, 319.
(154) Lehmann, K. K. *J. Chem. Phys.* **1992**, *96*, 1636.
(155) Page, R. H.; Shen, Y. R.; Lee, Y. T. *J. Chem. Phys.* **1988**, *88,* 4621.
(156) Scotoni, M.; Boschetti, A.; Oberhofer, N.; Bassi, D. *J. Chem. Phys.* **1991**, *94,* 971.
(157) Zhang, Y.; Kleppenstein, S. J.; Marcus, R. A. *J. Chem. Phys.* **1991**, *94*, 7319.
(158) Zhang, Y.; Marcus, R. A. *J. Chem. Phys.* **1992**, *97*, 5283.
(159) Utz, A. L.; Carrisquillo, E.; Tobiason, J. D.; Crim, F. F. *Chem. Phys.* **1995**, *190,* 311.
(160) Crim, F. F. *Annu. Rev. Phys. Chem.* **1993**, *44,* 397.
(161) Foy, B. R.; Casassa, M. P.; Stephenson, J. C.; King, D. S. *J. Chem. Phys.* **1990**, *92,* 2782 .
(162) Go, J.; Bethardy, G. A.; Perry, D. S. *J. Phys. Chem.* **1990**, *94*, 6153.
(163) Casassa, M. P.;Woodward, A. M.; Stephenson, J. C.; King, D. S. *J. Chem. Phys.* **1986,** *85,* 6235.
(164) (a) Matsumoto, Y.; Oshima, Y.; Takami, M. *J. Chem. Phys.* **1990**, *92,* 937. (b) Menoux, V.; LeDoucen, R.; Hauesler, C.; DeRoche, J. C. *Can. J. Phys.* **1984**, *62,* 322.
(165) Sun, H.; Watts, R. O.; Buck, U. *J. Chem. Phys.* **1992**, *96,* 1810.
(166) Quack, M.; Stohner, J.; Suhm, M. A. *J. Mol. Struct.* **1993**, *294,* 33.
(167) Michael, D. W.; Lisy, J. M. *J. Chem. Phys.* **1986**, *85,* 2528.
(168) Miller, R. E. Private communication.
(169) Davis, S.; Anderson, D. T.; Farrell, J. T., Jr.; Nesbitt, D. J. *J. Chem. Phys.*, in press.
(170) Gabrys, C. M.; Uy, D.; Jagod, M.-F.; Oka, T.; Amaro, T *J. Phys. Chem.* **1995**, *99*, 15611.
(171) Parmenter, C. S.; Stone, B. M. *J. Chem. Phys.* **1986**, *84,* 4710.
(172) Moss, D. B.; Parmenter, C. S.; Ewing, G. E. *J. Chem. Phys.* **1987**, *86,* 51.
(173) Zhao, Z.-Q.; Parmenter, C. S.; Moss, D. B.; Bradley, A. J.; Knight, A. E. W.; Owens, K. G. *J. Chem. Phys.* **1992**, *96,* 6362.
(174) Covelskie, R. A.; Dolson, D. A.; Parmenter, C. S. *J. Phys. Chem.* **1985**, *89,* 645.
(175) (a) Moss, D. B.; Parmenter, C. S. *J. Chem. Phys.* **1993**, *98,* 6897. (b) Timbers, P. J.; Parmenter, C. S.; Moss, D. B. *J. Chem. Phys.* **1994**, *100,* 1028.
(176) Walters, V. A.; Colson, S. D.; Snavely, D. N.; Wiberg, K. B.; Jamison, B. M. *J. Phys. Chem.* **1985**, *89*, 3857.
(177) Martens, C. C.; Reinhardt, W. P. *J. Chem. Phys.* **1990**, *93,* 5621.
(178) Tan, X.-Q.; Majewski, W. A.; Plusquellic, D. F.; Pratt, D. W. *J. Chem. Phys.* **1991**, *94,* 7721.
(179) (a) Lu, K.-T.; Weinhold, F.; Weisshaar, J. C. *J. Chem. Phys.* **1995**, *102,* 6787. (b) Richard, E.; Walker, R.; Weisshaar, J. C. *J. Chem. Phys.*, in press.
(180) Li, H.; Eyra, G. S.; Philips, L. A. *J. Chem. Phys.* **1992**, *97*, 5956.
(181) Chambers, C. C.; Thompson, D. L. *Chem. Phys. Lett.* **1994**, *218,* 166.
(182) Mehta, A.; Stuchebrukov, A. A.; Marcus, R. A. *J. Phys. Chem.* **1995**, *99*, 2677.
(183) Stuchebrukov, A. A.; Mehta, A.; Marcus, R. A. *J. Phys. Chem.* **1993**, *97*, 12491.

JP960698W